

**Integrated Master in Chemical Engineering**

***Synthesis and Electrochemical Properties of  
Ionic Liquids***

**Master Thesis**

of

**Amadeu Gomes Rocha**

Developed under the dissertation curricular unit

Accomplished in

**Technische Universität München**



Orientation in TUM: Prof. Dr. Fritz E. Kühn



Universidade do Porto  
Faculdade de Engenharia  
**FEUP**

**Chemical Engineering Department**

**July 2015**



This page is intentionally left blank





## Acknowledgements

Firstly, I would like to thank my grandmother, whose will to accompany me throughout my engineer course surpassed all barriers imposed by age. Also, to my parents, for giving me all the mental and affective support necessary for me to become a healthy individual.

I would also like to thank Joana Trindade, the fellow adventurer and best friend that everyone should have in life.

To Prof. Madeira, for the continuous incentive to students to pursuit an academic experience outside their homeland. I would also like to thank all of my professors at FEUP who were responsible for bringing me to this phase of my engineering degree.

To Prof. Dr. Kühn, I would like to thank his intuition for what international relations can do for scientific development and also for trusting and welcoming me into TUM.

In a more direct way, I would like to thank Robert Reich, Sara Abbassi and Dr. Iulius Markovits. To Robert, for introducing me to the world of experimental chemistry in the best way, to Sara, for all the technical advices given and to Iulius for the positive attitude always showed to me and my results.

I could never forget all the invisible work of the technical support, that provide TUM an organized functioning as a teaching facility and to all the inorganic group for the good mood and availability in helping others, which is fundamental in any work environment.

I would like to thank all my friends and colleagues, with their help all the obstacles were easier to surpass, I will be their reflexion as a future engineer.

To the Karate group in TS Jahn München club for providing me with my first professional experience, as well as the best possible welcome to Bavaria.

---

## Resumo

Os líquidos iônicos são sais com ponto de fusão inferior a 100 °C. As suas propriedades electroquímicas únicas fazem com que estes compostos sejam vistos como uma promessa em imensas áreas energéticas, nomeadamente na aplicação como eletrólitos em baterias de ião-lítio. Nesta tese foram sintetizados e caracterizados sete líquidos iônicos, [BMIm][TFSI], [BnMIm][TFSI], [Bn<sup>F</sup>MIm][TFSI], [BMIm][PF<sub>6</sub>], [BnMIm][PF<sub>6</sub>], [Bn<sup>F</sup>MIm][PF<sub>6</sub>] e [BnMIm][BF<sub>4</sub>]. Estes líquidos iônicos foram caracterizados com recurso a espectroscopia <sup>1</sup>H NMR, <sup>13</sup>C NMR, análise elementar e janela electroquímica. Dois dos líquidos iônicos foram purificados até altos níveis de pureza, os restantes atingiram também um nível não muito afastado do ideal. Os limites catódicos e anódicos obtidos permitiram sequenciar os catiões e os aniões por ordem de dimensão da janela electroquímica. A sequência de catiões obtida foi Bn<sup>F</sup>Mim<sup>+</sup> > BnMIm<sup>+</sup> > BMIm<sup>+</sup> enquanto que a sequência de aniões obtida foi PF<sub>6</sub><sup>-</sup> > BF<sub>4</sub><sup>-</sup> > TFSI<sup>-</sup>. A janela mais ampla foi obtida para uma solução 0.1 M de [BnMIm][PF<sub>6</sub>] com um valor de 7.05 V.

**Palavras-chave:** Líquidos iônicos, janela electroquímica, baterias ião lítio, catião, anião.

---

## Abstract

Ionic liquids are salts with a fusion point below 100 °C. Their unique electrochemical properties provide these compounds a view of promise in several energetic areas, namely in the application as electrolytes in lithium-ion batteries. In this thesis seven ionic liquids were synthesised and characterized, [BMIm][TFSI], [BnMIm][TFSI], [Bn<sup>F</sup>MIm][TFSI], [BMIm][PF<sub>6</sub>], [BnMIm][PF<sub>6</sub>], [Bn<sup>F</sup>MIm][PF<sub>6</sub>] and [BnMIm][BF<sub>4</sub>]. These ionic liquids were characterized with the help of <sup>1</sup>H NMR and <sup>13</sup>C NMR spectroscopy as well as elemental analysis and electrochemical window. Two of the ionic liquids were purified to a high degree of purity, and the remaining also achieved a level close to ideal. The cathodic and anodic limits allowed the sequence of the anions and cations by dimension order of the electrochemical window. The obtained cations sequence was Bn<sup>F</sup>Mim<sup>+</sup> > BnMIm<sup>+</sup> > BMIm<sup>+</sup> as the anion sequence was PF<sub>6</sub><sup>-</sup> > BF<sub>4</sub><sup>-</sup> > TFSI<sup>-</sup>. The wider window was obtained for a 0.1 M solution of [BnMIm][PF<sub>6</sub>] with a value of 7.05 V.

**Key words:** ionic liquids, electrochemical window, li-ion batteries, cation, anion.

---





## Declaration

I hereby declare under commitment of honour, that this work is original and that all its non-original contributions are duly referenced with source identification.

*Amadeu Gomes Rocha, July 2015*

# Table of contents

<b>1</b>	<b>Introduction.....</b>	<b>1</b>
1.1	Theoretical introduction .....	1
1.1.1	Battery, a brief history.....	1
1.1.2	The battery functioning.....	3
1.1.3	Ionic liquids: a brief history and electrochemical applications.....	4
1.1.4	Electrochemical tests .....	8
1.2	Proposed objectives .....	9
1.3	Thesis structure .....	10
<b>2</b>	<b>Context and State of the Art .....</b>	<b>11</b>
<b>3</b>	<b>Technical Description .....</b>	<b>13</b>
3.1	Chemicals used in the synthesis of the ionic liquids .....	13
3.2	Methods .....	14
3.3	Procedure .....	15
3.3.1	Bromides synthesis.....	15
3.3.2	Anion Substitution .....	16
3.3.3	Electrochemical tests .....	19
<b>4</b>	<b>Results and discussion .....</b>	<b>21</b>
4.1	Products characterization.....	21
4.1.1	Bromides spectrums .....	21
4.1.2	Final ILs characterization.....	23
4.2	Electrochemical tests results .....	29
4.2.1	EW overview .....	32
<b>5</b>	<b>Conclusions .....</b>	<b>35</b>
	<b>References .....</b>	<b>37</b>
	<b>Annex 1.....</b>	<b>41</b>
	<b>Annex 2.....</b>	<b>42</b>
	<b>Annex 3.....</b>	<b>43</b>

Annex 4.....	53
--------------	----

# Figure Index

Figure 1. Battery discharging (left) and charging (right)	4
Figure 2. Number of publications dealing with ionic liquids since 2001	4
Figure 3. Ethylammonium nitrate molecule	5
Figure 4. 1-butylpyridinium tetrachloroaluminat	5
Figure 5. Typical cations and anions from each generation of ILs.	6
Figure 6. Cations and anions of the synthesized and characterized ILs	9
Figure 7. Scheme with the bromides reactions.	15
Figure 8. Anions of the salts used for the anions substitutions	17
Figure 9. [BMIm][Br] Molecule	21
Figure 10. [BnMIm][Br]	22
Figure 11. [Bn <sup>F</sup> MIm][Br]	22
Figure 12. [BMIm][TFSI]	23
Figure 13. [BnMIm][TFSI]	24
Figure 14. [Bn <sup>F</sup> MIm][TFSI]	25
Figure 15. [BMIm][PF <sub>6</sub> ]	26
Figure 16. [BnMIm][PF <sub>6</sub> ]	26
Figure 17. [Bn <sup>F</sup> MIm][PF <sub>6</sub> ]	27
Figure 18. [BnMIm][BF <sub>4</sub> ]	28
Figure 19. LSV graph of Blank LiPF <sub>6</sub>	29
Figure 20. LSV graph of [BnMIM][PF <sub>6</sub> ] 0.10 M (2nd trial).	29
Figure 21. LSV graph of [BnMIM][PF <sub>6</sub> ] 0.1 M (2nd trial) and Blank LiPF <sub>6</sub>	30
Figure 22. State of the art of the electrochemical windows of ILs	41
Figure 23. NMR spectrum of [BMIm][Br] <sup>1</sup> H	43
Figure 24. NMR spectrum of [BMIm][Br] <sup>13</sup> C	43
Figure 25. NMR spectrum of [BnMIm][Br] <sup>1</sup> H	44
Figure 26. NMR spectrum of [BnMIm][Br] <sup>13</sup> C	44

---

Figure 27. NMR spectrum of $[\text{Bn}^{\text{F}}\text{MIm}][\text{Br}]$ $^1\text{H}$	45
Figure 28. NMR spectrum of $[\text{Bn}^{\text{F}}\text{MIm}][\text{Br}]$ $^{13}\text{C}$	45
Figure 29. NMR spectrum of $[\text{BMIm}][\text{TFSI}]$ $^1\text{H}$	46
Figure 30. NMR spectrum of $[\text{BMIm}][\text{TFSI}]$ $^{13}\text{C}$	46
Figure 31. NMR spectrum of $[\text{BnMIm}][\text{TFSI}]$ $^1\text{H}$	47
Figure 32. NMR spectrum of $[\text{BnMIm}][\text{TFSI}]$ $^{13}\text{C}$	47
Figure 33. NMR spectrum of $[\text{Bn}^{\text{F}}\text{MIm}][\text{TFSI}]$ $^1\text{H}$	48
Figure 34. NMR spectrum of $[\text{Bn}^{\text{F}}\text{MIm}][\text{TFSI}]$ $^{13}\text{C}$	48
Figure 35. NMR spectrum of $[\text{BMIm}][\text{PF}_6]$ $^1\text{H}$	49
Figure 36. NMR spectrum of $[\text{BMIm}][\text{PF}_6]$ $^{13}\text{C}$	49
Figure 37. NMR spectrum of $[\text{BnMIm}][\text{PF}_6]$ $^1\text{H}$	50
Figure 38. NMR spectrum of $[\text{BnMIm}][\text{PF}_6]$ $^{13}\text{C}$	50
Figure 39. NMR spectrum of $[\text{Bn}^{\text{F}}\text{MIm}][\text{PF}_6]$ $^1\text{H}$	51
Figure 40. NMR spectrum of $[\text{Bn}^{\text{F}}\text{MIm}][\text{PF}_6]$ $^{13}\text{C}$	51
Figure 41. NMR spectrum of $[\text{BnMIm}][\text{BF}_4]$ $^1\text{H}$	52
Figure 42. NMR spectrum of $[\text{BnMIm}][\text{BF}_4]$ $^{13}\text{C}$	52
Figure 43. EWs comparison between $[\text{BnMIm}][\text{BF}_4]$ , $[\text{BnFMIm}][\text{TFSI}]$ and $[\text{BMIm}][\text{TFSI}]$	53

## Table Index

<i>Table 3. State of the art for ILs EWs</i>	12
<i>Table 2. Chemicals used in the synthesis of ILs</i>	13
<i>Table 3. Weights of used reactants for the bromides synthesis</i>	16
<i>Table 4. Weights of used reactants for the anions substitutions</i>	17
<i>Table 5. Weights for the LSV solutions</i>	19
<i>Table 6. Data imputted in Gamry framework software</i>	20
<i>Table 7. LSV EWs results.</i>	31
<i>Table 8. Average values for the same cation and concentration</i>	32
<i>Table 9. Average values for BnMIm cation, same anion and concentration</i>	33
<i>Table 10. Average values for the same anion and concentration</i>	33
<i>Table 11. Summary of the final anion substitution reaction appearance, extraction method and final IL appearance.</i>	42
<i>Table 12. Full LSV results</i>	54



# List of abbreviations

$\delta$	chemical shift
A	Ampere
ACM	active charcoal method
AL	anodic limit
CE	counter electrode
CL	cathodic limit
CV	cyclic voltammetry
DCM	dichloromethane
e.g	for example
EVs	electric vehicles
EW	electrochemical window
Fig.	figure
GC	glassy carbon
HEVs	hybrid-electric vehicles
IL	ionic liquid
LSV	linear sweep voltammetry
M	molar
mbar	millibar
MHz	megahertz
mL	millilitre
m.p	melting point
n.a	not analysed
NiCd	Nickel-Cadmium battery
ppm	parts per million
NMR	nuclear magnetic resonance
NTU	Nanyang Technological University



QRE	quasi reference electrode
R	organic rest
RE	reference electrode
r.t.	room temperature
Tab.	table
TUM	Technical University of Munich
U.S	United States
WE	working electrode
V	Volts

# List of ionic liquids and other chemicals

[BMIm][Br]	1-Butyl-3-methylimidazoliumbromide
[BnMIm][Br]	1-Benzyl-3-methylimidazoliumbromide
[Bn <sup>F</sup> MIm][Br]	2,3,4,5,6-Pentafluorobenzyl-3-methylimidazoliumbromide
[BMIm][PF <sub>6</sub> ]	1-Butyl-3-methylimidazolium hexafluorophosphate
[BnMIm][PF <sub>6</sub> ]	1-Benzyl-3-methylimidazolium hexafluorophosphate
[Bn <sup>F</sup> MIm][PF <sub>6</sub> ]	2,3,4,5,6-Pentafluorobenzyl-3-methylimidazolium hexafluorophosphate
[BMIm][TFSI]	1-Butyl-3-methylimidazolium bis(trifluormethansulfonyl)imide
[BnMIm][TFSI]	1-Benzyl-3-methylimidazolium bis(trifluormethansulfonyl)imide
[Bn <sup>F</sup> MIm][TFSI]	2,3,4,5,6-Pentafluorobenzyl-3-methylimidazolium bis(trifluormethansulfonyl)imide
[BMIm][BF <sub>4</sub> ]	1-Butyl-3-methylimidazolium tetrafluoroborate
[BnMIm][BF <sub>4</sub> ]	1-Benzyl-3-methylimidazolium tetrafluoroborate
[Bn <sup>F</sup> MIm][BF <sub>4</sub> ]	2,3,4,5,6-Pentafluorobenzyl-3-methylimidazolium tetrafluoroborate
[PMIm][TFSI]	Methylimidazoliumbis(trifluoromethylsulfonyl)imide
BnBr	Benzyl bromide
<sup>F</sup> BnBr	2,3,4,5,6-Pentafluorobenzyl bromide
BuBr	Butyl bromide
MIm	1-Methylimidazole
MImBr	1-Methylimidazoliumbromide
BuBr	Butyl bromide
LiPF <sub>6</sub>	Lithium hexafluorophosphate
[EtNH <sub>3</sub> ][NO <sub>3</sub> ]	Ethylammonium nitrate
BF <sub>4</sub>	Tetrafluoroborate
PF <sub>6</sub>	Hexafluorophosphate

TFSI	Bis(trifluoromethansulfonyl)imide
LiTFSI	Lithium bis(trifluoromethansulfonyl)imide
BMIm	1-Butyl-3-methylimidazole
BnMIm	1-Benzyl-3-methylimidazole
Bn <sup>F</sup> MIm	2,3,4,5,6-Pentafluorobenzyl-3-methylimidazole
Fe	Ferrocene
NH <sub>4</sub> PF <sub>6</sub>	Ammonium hexafluorophosphate
NH <sub>4</sub> BF <sub>4</sub>	Ammonium tetrafluoroborate
DCM	Dichloromethane
MgSO <sub>4</sub>	Magnesium sulfate

# 1 Introduction

## 1.1 Theoretical introduction

### 1.1.1 Battery, a brief history

Electricity can be viewed as one of the most important discoveries of Mankind since fire. It is easy to assume that humans were aware of its existence for a long time, since it is observable in natural phenomena such as thunderstorms or electric fishes, but there is some disagreement about when humans were capable of producing electricity. Some believe that the called Parthian Battery, dated around 2000 years ago, was indeed a battery. After all, the main components of a battery were found nearby; a clay jar once filled with some acid, like vinegar (electrolyte), an iron rod (positive terminal) covered by a copper cylinder (negative terminal) is known to be capable of producing from 1.1 to 2.0 Volts (V) [1].

It is not fully accepted that the Parthians were already using the Parthian Jar as a battery, perhaps it was only an hermetical vessel to store important scrolls, where the paper could decompose leaving a trace of acidic organic residue inside [2].

In the beginning of the 19<sup>th</sup> century, Alessandro Volta gave one of the first public demonstrations of electricity. Volta figured out that two different metals in the presence of some fluids would create a continuous electric effect. By feeling that effect with his own tongue, and trying different combinations of metals, Volta sorted them by electric potential. After Volta discovered that the presence of an acid would increase the so called “electric effect” he constructed the “first official device to create an electric current for a length of time”, the battery. It consisted of a column of copper coins (anode) alternated with plates of zinc (cathode) separated by leather soaked with salt (electrolyte). Volta’s work awarded him a Copley Medal from the Royal Society of London, and the interest of Napoleon Bonaparte, which boosted the interest of other scientists in trying to improve the Volta’s battery [1, 3].

In the same beginning of century, in the year 1800, Sir Humphry Davy discovered the principles of electrolysis. Two years later William Cruickshank designed a squared sealed version of the battery similar to the flooded battery that we use today. With this design it was possible to provide more energy than the Volta’s discs battery and did not suffer from drying out. The drying out effect refers to the hydrolysis that comes from the normal use of

batteries or an overcharge that splits the water into hydrogen and oxygen [1] [4, 5]. Later in 1859 the physicist Gaston Planté invented the first rechargeable battery, based in lead-acid. This device has a low energy density but very high current intensity, which does not suffer from memory effects and can recharge itself with accumulators. Due to the advantageous factors, this kind of battery is still used in starting, lighting and ignition batteries in cars [6, 7].

The nickel-cadmium battery (NiCd) was later invented in 1899 by the Swedish Waldemar Jungner as an alternative for the lead-acid batteries. However, it was only later in 1932 that Shlecht and Ackerman achieved satisfactory load currents and improved longevity of NiCd with the invention of the sintered pole plate. This new kind of battery was only available to commercial usage in 1947 when Georg Neumann sealed the cell. This made it possible to apply rechargeable batteries in portable applications due to the fast charging, high number of charge/discharge cycles and the good low temperature performance. With the NiCd growing in the market, there was the environmental problem associated with this new kind of batteries toxicity. This undesirable characteristic soon urged the necessity to change to Nickel-metal hydride batteries, which was the first step to the introduction of Li-ion batteries in the market in 1991 [1].

The Li-ion batteries were being studied since 1976 [8], although they were only introduced in the market after it was proven that the use of an anode with intercalated carbon/graphite could eliminate the problems of poor lithium metal rechargeability; this greatly improved the safety of the battery system. For this major step in the history of batteries the work of J.O. Besenhard at the Technical University of Munich (TUM) was very important. In the 70s, while there were being done numerous researches about lithium batteries, J.O Besenhard was studying the reversible alkali metal ion intercalation into graphite (anodes) [9] and oxide materials (cathodes)[10]. Soon he proposed his work to be introduced in lithium batteries [11, 12].

Followed by the work of Goodenough, which used lithium cobalt oxide ( $\text{LiCoO}_2$ ) as a cathode material for the first time, and the Yazami's, who discovered the graphite electrode used in commercial lithium it was possible for Sony<sup>TM</sup> in 1991 to commercialize the first Li-ion battery [13].

This new kind of batteries revolutionized the market of rechargeable batteries. They had a higher energy density, need not periodical maintenance, the self-discharge was less than half of the nickel based batteries and they did not need to be discharged completely before charging. Furthermore, these batteries appeared not in a fully matured state, and its constitution has been improving on a continuing basis since their appearance [13].

Nowadays the biggest challenge of Li-ion batteries is the entrance in the electric vehicles (EVs) and hybrid-electric vehicles (HEVs) market. For that purpose improvements should be done in terms of safety, cost and performance. One of the ways to achieve this purpose could be the replacement of the State of the art organic liquid electrolytes with solid electrolytes. This would enable high energy and an intrinsically safe cell design. However the already existing electrolytes of this kind cannot be implemented in real-time practical applications due to their narrow electrochemical window or low ionic conductivity [14]. Another possible solution for the safety and performance problems is the substitution of the used carbonate based solvents by ionic liquids (ILs).

### 1.1.2 The battery functioning

To each chemical species there is an associated energy, this energy, entitled as chemical energy, is present in every molecular bond. As with all chemical reactions, there is a reactant turning into a product with a different energy value. It is comprehensible that science developed ways to use this energy present in all molecules for its own use. A battery is precisely one of those devices. In its basic constitution there is a negative and a positive electrode. While discharging, the battery negative electrode is an anode where oxidation occurs. Meanwhile the positive electrode is a cathode, where there is a reduction process. By making the released electrons pass from one electrode to the other by an external circuit electric energy is produced. The separation of two electrodes is gathered with an electrolyte, which acts as electronical insulant as well as an ionic conductant. This way the electric current is separated from the ionic current since only the positive ions formed on the electrodes can go through the electrolyte [15, 16]. When recharging a battery, electric energy is given to the system, making the electrons flow into the opposite direction. This is only possible if the oxidation-reduction reactions are reversible in both electrodes. If so, the chemical species return to their original state, before discharging. A schematic figure can be seen in the Fig. 1.

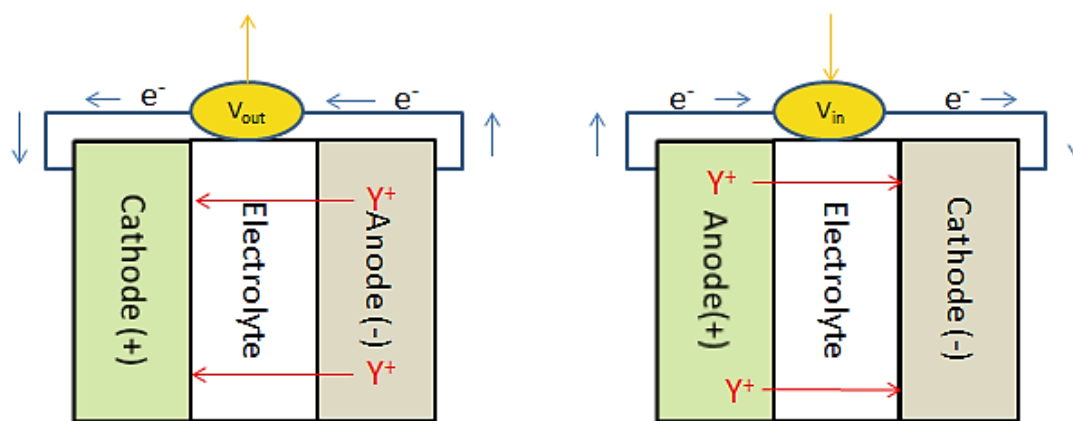


Figure 1 Battery discharging (left) and charging (right).

### 1.1.3 Ionic liquids: a brief history and electrochemical applications

By convention, ionic liquids are labelled as salts with melting points below 100°C. The number of publications about ILs has been increasing year by year since the beginning of the millennium (Fig. 2). The increase in academical interest is correlated with the potential advantages that ILs can offer to different industries [17].

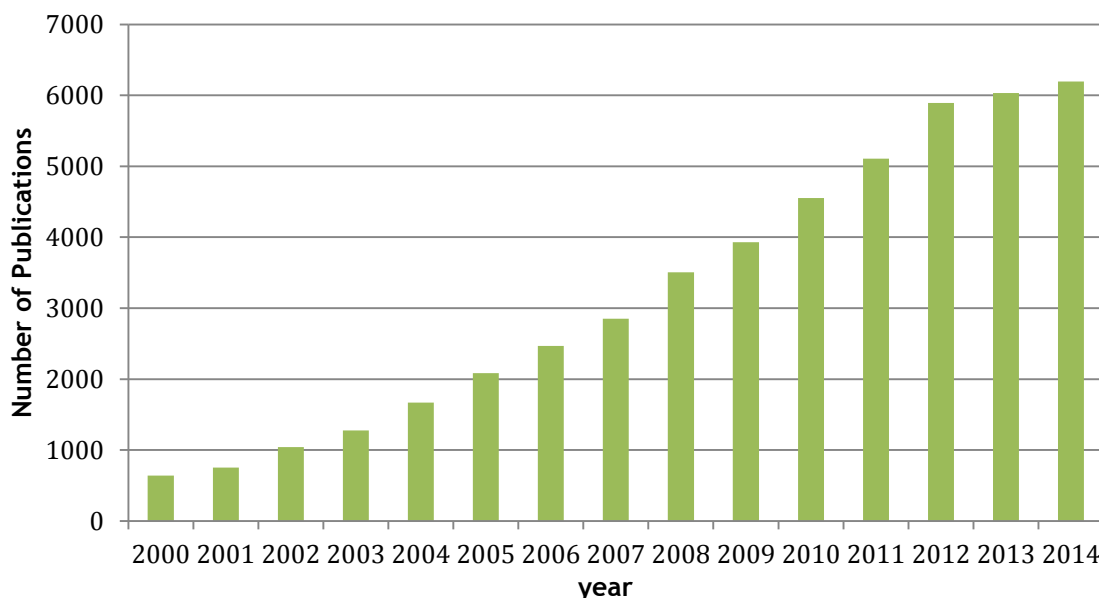


Figure 2. Number of publications dealing with ionic liquids since 2001 [17].

Being the successors of the high temperature molten salts, ILs do not have the inconvenience of needing high operational temperatures which make industrial processes very expensive due to energy necessities. It was in 1914 the first time an IL was synthesized deliberately for its ionic character, in that time Paul Walden prepared ethylammonium

nitrate (m.p 12°C)  $[\text{EtNH}_3][\text{NO}_3]$ , which was later studied in extensive detail [18]. This molecule can be seen in Fig.3.

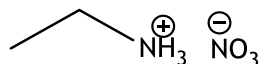


Figure 3. Ethylammonium nitrate molecule.

Later in 1963, the U.S. Air Force Academy tried to find more adequate electrolytes for thermal batteries and intensified the research on ILs. Their first result was a chloroaluminate developed from a mixture of alkali halides and aluminium chloride [19].

But it was only 15 years later that the era of ionic liquids really started. In 1978 Gale *et al.* synthesized the 1-butylpyridinium tetrachloroaluminate,  $(\text{C}_9\text{H}_{14}\text{AlCl}_4\text{N})$  Fig. 4. This point marked an overturn since it stimulated great interest to chemists trying to improve the properties of this new IL [20].

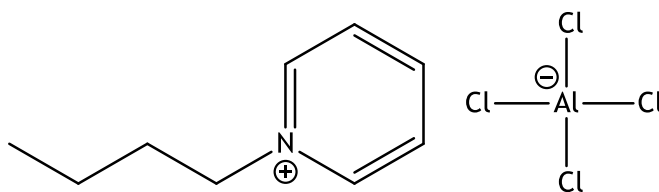


Figure 4. 1-butylpyridinium tetrachloroaluminate.

However, one of the disadvantages of the pyridinium and imidazolium based chloroaluminate was the production of hydrochloric acid in presence of water, which was avoided firstly in 1992 when Zaworotko *et al.* had the idea to synthesize salts with dialkylimidazolium cations and water-stable anions. This led to the substitution of the water sensitive tetrachloroaluminate by the more stable tetrafluoroborate  $(\text{BF}_4^-)$ , hexafluorophosphate  $(\text{PF}_6^-)$ , nitrate  $(\text{NO}_3^-)$ , sulfate  $(\text{SO}_4^{2-})$  and acetate salts  $(\text{C}_2\text{H}_3\text{O}_2^-)$  [21].

Although these compounds were first regarded as potential electrolytes for batteries by Zaworotko *et al.* these new ionic liquids were more useful in other applications [19]. This step ended the first generation of ILs and marked the beginning of the generation of non-aluminate ILs or second generation ILs.

The synthesis of the hydrophobic dialkylimidazolium ILs with the bis(trifluoromethanesulfonyl)imide (TFSI)  $(\text{C}_2\text{F}_6\text{NO}_4\text{S}_2^-)$  anions was described by Bonhôte *et al.* in 1996 [22]. The third generation of ionic liquids appeared around the 2000s and is comprised of the task-specific ionic liquids and chiral ionic liquids [23].



Assembling the ILs in generations is only a way to order the chronological research focus of ILs. There are other ionic liquids which do not fit in these groups such as the previously mentioned ethylammonium nitrate [23]. In Fig. 5 are shown typical cations and anions from each generation of ILs.

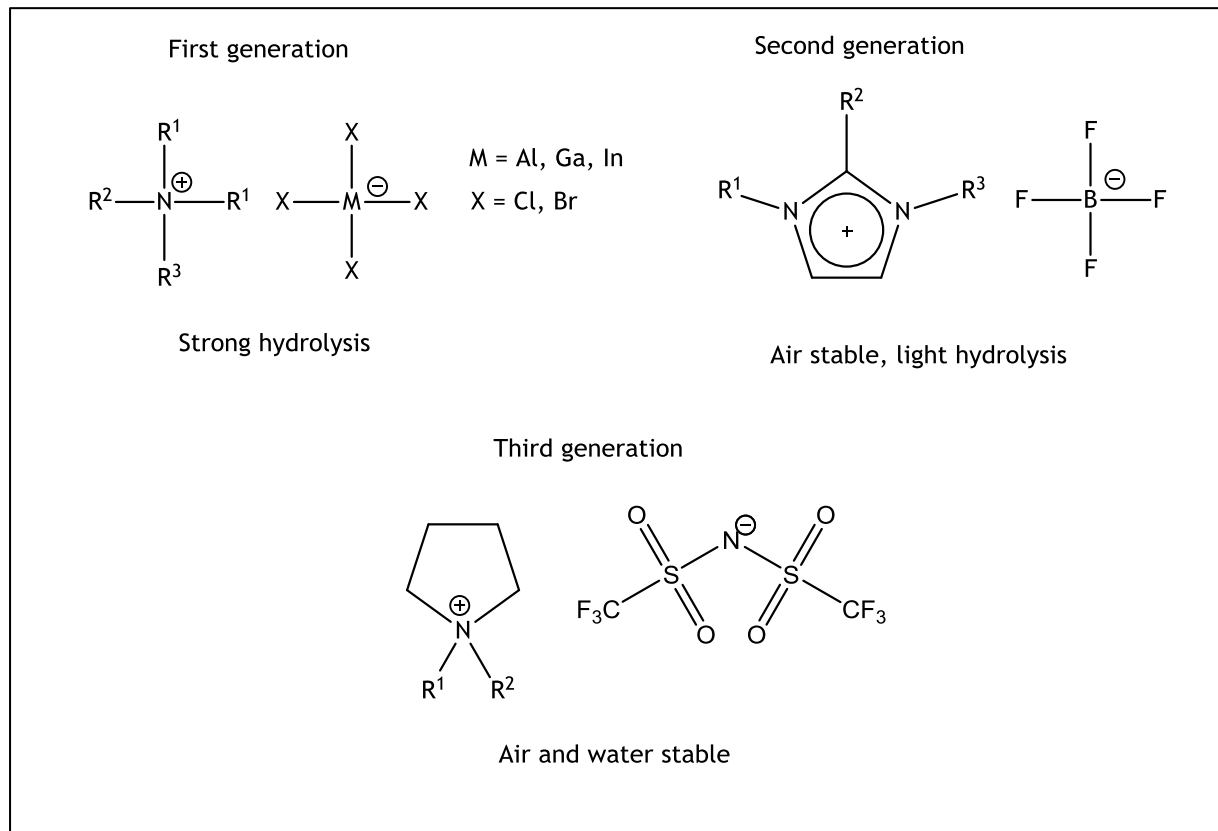


Figure 5. Typical cations and anions from each generation of ILs.

One of the most important characteristics in the added value of ILs is their highly flexible nature made possible by the diversity of anion-cation combinations and different modes of preparation. This enables a rational design of ILs to fine-tune their physical and chemical properties for a wide range of applications [24].

In fact ILs are viewed as novel and propitious materials for their wide range of useful physical and chemical properties, such as: thermal and electrochemical stability, low vapor pressure, electric conductivity, interesting solvent properties, possible biphasic systems, liquid crystalline structures, high heat capacity, non-flammability and electroelasticity. All these properties illustrate that ILs are suitable compounds for various applications, e.g: electrolytes, catalysis, separation technologies [25], lubricants [26], heat storage [27] and analytic chemistry [28, 29].

ILs were considered for some time as rather green solvents, as they are non-flammable, have a negligible vapour pressure and excellent thermal and chemical stability compared to

common used volatile organic solvents [14]. However recent studies revealed that their solubility in water and high chemical stability can be a problem in the future if correct ways of disposal and recycling are not developed [30].

Since their development that ILs are assumed as a possibility for the use in electrochemical applications. Their wide electrochemical window, high conductivity and unmeasurable vapour pressure up to 200° C are the key features for ionic liquids, which surpass the aqueous or other organic media in this area [31].

As it was mentioned in the previous section, at this point it is easy to understand why ILs as highly stable electrolytes for lithium batteries can be the missing key in the EVs and HEVs market. However, it is important to have in mind that the relatively high viscosity and cost of these compounds can be a limiting factor, as the ionic mobility and therefore the ionic conductivity is crucial. Literature already showed that this problem was taken into account, for instance, Kim *et al.* in 2010 synthesized the 1-propyl-3-methylimidazoliumbis(trifluoromethylsulfonyl)imide [PMIm][TFSI] ( $C_9H_{13}F_6N_3O_4S_2$ ) complexed with LiTFSI, where electrolyte showed a high ionic conductivity at room temperature [32]. To overcome both issues of cost and rate capability, studies in blended systems of ILs with conventional carbonate based electrolytes are becoming more common [33, 34].

There are also other electrochemical applications where the synthesis of ILs with better electrochemical properties, namely the electrochemical window (EW), can be of value. Electrodeposition is an essential technique where an electric current reduces dissolved deposited metal cations. It is used in several industries e.g. optical, sensorial, automotive and aerospace. The already aqueous existing solutions have the drawback of having a narrow EW (+/- 4V) hindering the deposition of metals with large negative reduction potentials [35]. The wider electrochemical window observed in some ILs, up to 6 V or even more, is a good promise for the electrodeposition of metals and semiconductors, and displays great potential in electroplating. In particular highlight are the TFSI,  $BF_4$  and  $PF_6$  anions (which are part of the ILs synthesized and characterized in this thesis) which are stable below the  $Li/Li^+$  reductive region, enabling its deposition [36, 37].

The electrochemical and solvent properties of ILs already showed to be useful in electrosynthesis and electrocatalysis. They open new ways for increased reactivity of processes and stability of reactants/products in ionic liquids [37]. Wei *et al.* in 2007 used the 1-Butyl-3-methylimidazoliumhexafluorophosphate [BMIm][ $PF_6$ ]( $C_8H_{15}F_6N_2P$ ) as a binder in the construction of a carbon paste electrode. The presence of the IL on this electrode increased the electro transfer rate and provided a biocompatible interface [38].

Recently, Van Aken *et al.* proposed a method to expand the EW of electrochemical capacitors by using electrochemical cells based on two identical onion-like carbon electrodes

and two different commercially available IL electrolytes and their mixtures in different ratios. On the paper is shown that the asymmetric behaviour of the electrolyte cation and anion toward the two electrodes limits the EW of the cell and therefore its energy density. A solution for this problem was proposed by formulating the IL electrolyte mixtures ratios in a way that balances the capacitance of the electrodes in a symmetric supercapacitor. This study can open a new way of research on the improvement of the energy density of supercapacitors and batteries [39].

#### 1.1.4 Electrochemical tests

As electrochemical applications operate under a certain electric potential it is natural that all components of the device need to support the voltage in which the device operates. Therefore the electrochemical window, or operating potential window, is one of the most important electrochemical properties to be identified in solvents and electrolytes used in electrochemical applications [40].

The EW can be defined as the difference between the cathodic limit (CL) and anodic limits (AL), which are the potentials in which the reduction and oxidation of the compound occurs, respectively.

In some applications such as the supercapacitors, the window is a significant factor. While in other applications, for instance the Li-ion batteries, it is the cathodic limit relative to the  $\text{Li}/\text{Li}^+$  that determines whether the solvent is reduced by lithium or not, while the anodic limit determines the voltage tolerable by the cathode [41]. As for ILs, generally the CL is set by the reduction of the cations and the AL by the oxidation of the anions [42].

The narrow EW of actual electrolytes is one of the factors preventing the potential of high-voltage cathodes with higher power density [41]. The discovery of compounds with wider EWs is one of the aspiring goals between researchers of ionic liquids. The methods commonly used to determine the ILs EWs are the linear sweep voltammetry (LSV) and the cyclic voltammetry (CV).

CV is a very powerful technique and one of the most commonly used electrochemical methods. With it the current is measured at the working electrode as the potential is changed as a linear function of time. The data is then plotted as potential vs. current and at the end of one measurement the potential scan is reversed making a new scan.

The LSV is a simpler technique and uses the same principle as CV, although in LSV the current is plotted once between a selected initial potential to a selected final potential [43]. Usually

in an electrochemical measurement an electrochemical cell and three electrodes are needed; a working electrode (WE), a reference electrode (RE) and a counter electrode (CE). The working electrode acts as a cathode or anode depending on the voltage being applied. The current flow is then measured between the working and counter electrode. The reference electrode has a constant and known potential which is used to measure the potential at where the redox reaction occurs. The potential is measured between the WE and the RE [44].

## 1.2 Proposed objectives

Following these assumptions the ILs that will be synthesized and characterized in this work have the following cations 1-butyl-3-methylimidazole ( $\text{BMIm}^+$ ) ( $\text{C}_8\text{H}_{15}\text{N}_2^+$ ), 1-benzyl-3-methylimidazole ( $\text{BnMIm}^+$ ) ( $\text{C}_{11}\text{H}_{13}\text{N}_2^+$ ), 2,3,4,5,6-Pentafluorobenzyl-3-methylimidazole ( $\text{Bn}^{\text{F}}\text{MIm}^+$ ) ( $\text{C}_{11}\text{H}_8\text{F}_5\text{N}_2^+$ ) and anions  $\text{TFSI}^-$ ,  $\text{BF}_4^-$ ,  $\text{PF}_6^-$ . Their chemical structures are represented in the Fig. 6.

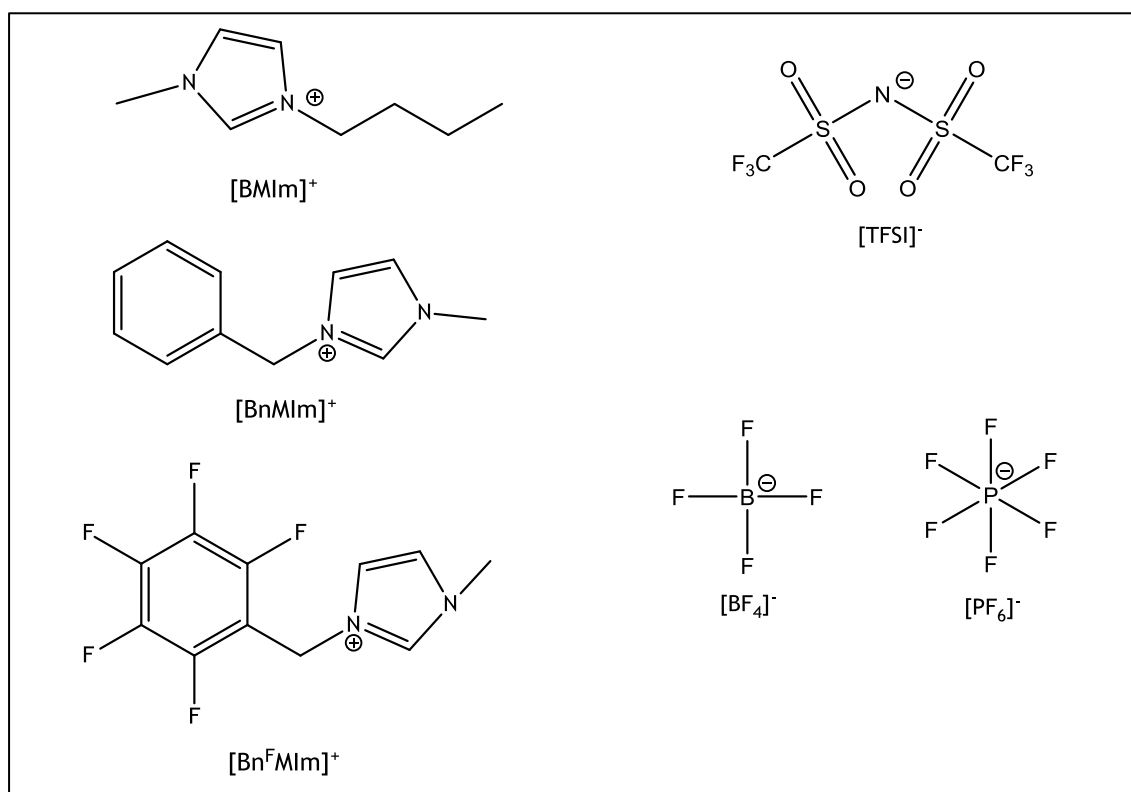


Figure 6. Cations and anions of the synthesized and characterized ILs.

Their characterization will be done by  $^1\text{H}$ -nuclear magnetic resonance (NMR),  $^{13}\text{C}$ -NMR and elemental analysis. The EW of each synthesized IL will be characterized with two different concentrations of IL 0.10 molar (M) and 0.25 M.

### 1.3 Thesis structure

In this chapter was given a theoretical introduction where it was explained how science evolved into the present work. The following chapter, “Context and State of the Art”, a brief context and perspective on ILs is done. The TUM and NTU approach to this field that lead to the topic for this thesis is also mentioned. Finally, a summary of a review paper is presented that refers to the state of the art in reported ILs EWs so far.

In the technical description chapter the experimental accomplished work is presented with all the necessary information for its reproducibility. Theoretical data is also included in the not so obvious steps.

The posterior chapter, “Results and discussion” is focused in the experimental results and their interpretation. When the obtained outcome was not as expected, the more likely reasons were given for these unpredicted results.

As the last chapter, conclusions of all the accomplished work are given, with a self-valuation of the efforts and results done, enunciating in a succinct manner the results and the advantages they present to the teaching institution. Future steps in this field will also be addressed.

## 2 Context and State of the Art

One of the biggest challenges of present day science is the joint action of efficiency and sustainability in the development of new technologies. The necessity to create large-scale and sustainable energy storage solutions to decrease the fossil fuels consumption is one of the greatest priorities in this field. The development of more stable and less pollutant electrolytes would be a big step towards a “greener” future energy system.

The work presented in this thesis occurred through a partnership between the Technische Universität München and the Energy Research Institute of the Nanyang Technological University (NTU). Its main goal is to find a suitable IL to act as an electrolyte in high potential batteries. To this end different ILs were synthesized and their electrochemical windows were characterized.

As was already stated, the ILs used for energy applications is a hot topic of research in the field and therefore institutes have been increasing their focus on these promising compounds. The research is already advanced in NTU but little information was shared about the subject due to confidentiality reasons.

At TUM this topic is rather new. As the work was done at the chair of molecular catalysis, the ILs were previously used as solvents and catalysts rather than electrolytes [45]. Now the research group lead by Prof. Kühn started to synthesize different ILs, in order to study their behaviour as electrolytes.

A reference article found with the state of the art was done by Can-can *et al.* and consists in a review of ILs EWs tested so far. Though the paper is written in Mandarin, the abstract, tables and figures are reported in English [46].

In the tables, that can be fully seen in the Fig. 22 in the Annex 1 is possible to see that the BMIm cation is the cation with most ILs EWs reported so far. There are numerous studies done with different working electrodes and reference electrodes. The authors categorize the results and conclude the following qualitative order sequences: The EW size depends on the type of used WE and tends to follow the order  $W > GC > Pt \approx Au$ . The cathodic limiting potential of ionic liquids tends to decrease in the following order: ammonium  $\approx$  phosphonium  $>$  pyrrolidinium  $>$  piperidinium  $\approx$  morpholinium  $>$  azepanium  $\approx$  imidazolium  $>$  sulfonium  $>$  pyridinium. The anodic limiting potential of ILs tend to follow the sequence:  $TFSI^- \approx R_FBF_3^- > BF_4^- > TSAC^- > F(HF)_{2,3}^- > CF_3COO^- > HCOO^-$

In the table reported by Can-can *et al.* is also possible to notice a problem in researches done in this area. Different potential reference scales are constantly used when

testing the EWs of ILs, which makes difficult to establish a convincing sequence of electrochemical stability for all cation and anion combinations [40, 47].

In the Fig. 22 it is not possible to find the same electrodes combinations as the ones used in this thesis. A selection of groups with the same electrodes can be seen in the Tab. 1 for three different ILs with the three different anions present in this work. The coupled cation is also present in this thesis and is the same in all the ILs. The glassy carbon (GC) as WE and Pt quasi reference electrode (QRE) as RE data are the values that can be used to compare the three ILs. In the same table is also shown the wider EW reported for each of the three ILs; however this values cannot be used to comparison since the same electrodes were not used to perform the tests.

Table 1. State of the art for ILs EWs. <sup>a</sup>[48] <sup>b</sup>[46] <sup>c</sup>[49]

Ionic liquid	Working electrode	Reference electrode	CL(V) Vs.RE	CL(V) Vs. Fe/Fe <sup>+</sup>	AL(V) Vs.RE	AL (V) Vs.Fe/Fe <sup>+</sup>	EW
[BMIm][TFSI]	Pt			-2.70		2.30	5.00 <sup>a</sup>
[BMIm][TFSI]	GC	Pt QRE	-2.40		2.50		4.90 <sup>b</sup>
[BMIm][PF <sub>6</sub> ]	GC	Pt QRE	-2.50		3.85		6.35 <sup>c</sup>
[BMIm][PF <sub>6</sub> ]	W	Pt QRE	-2.10		5.00		7.10 <sup>c</sup>
[BMIm][BF <sub>4</sub> ]	GC	Pt QRE	-1.80		3.65		5.45 <sup>c</sup>
[BMIm][BF <sub>4</sub> ]	W	Pt QRE	-1.60		4.50		6.10 <sup>c</sup>

A QRE has a potential that can swing between experiments. The potential for a silver QRE, like the one used in this thesis, can swing by at least 200 mV between experiments within the same IL [50]. Because of its ideal reversible behaviour, the oxidation of ferrocene (Fe) is used in CV and LSV studies as a mean of reference electrode potential calibration [51]. No literature was found with the EWs of ILs with the BnMIM and Bn<sup>F</sup>MIm as cations, so the present work can have the first results reported for these ions.

### 3 Technical Description

#### 3.1 Chemicals used in the synthesis of the ionic liquids

All the chemicals used for the synthesis of the ILs can be seen on the following Tab. 2:

*Table 2. Chemicals used in the synthesis of ILs.*

Substance	Manufacturer	Purity [%]
1-methylimidazole	abcr GmbH	99
1-bromobutane	Sigma Aldrich	99
Toluene	Acros	99
Magnesium sulfate hydrate	Riedel-de H��en	99
Lithiumbis(trifluormethansulfonyl)imide	Acros	99
Benzyl bromide	Sigma Aldrich	98
2,3,4,5,6-pentafluorobenzyl bromide	Sigma Aldrich	99
Ammonium hexafluorophosphate	Sigma Aldrich	>98
Ammonium tetrafluoroborate	Acros	99
Litium hexafluorophosphate solution 1M	Sigma Aldrich	50



## 3.2 Methods

The  $^1\text{H}$  (400 MHz) and  $^{13}\text{C}$  (100 MHz) spectrums were performed by a 400 MHz Bruker Advance DPX-400 Spectrometer. The solvent signals used as internal standards to evaluate the synthesized chemicals were  $\text{CDCl}_3$  ( $^1\text{H}$ :  $\delta=7.26$  ppm;  $^{13}\text{C}$ :  $\delta=77.16$  ppm),  $\text{DMSO-d}_6$  ( $^1\text{H}$ :  $\delta=2.50$  ppm;  $^{13}\text{C}$ :  $\delta=39.52$  ppm) and  $\text{CD}_3\text{CN}$  ( $^1\text{H}$ :  $\delta=1.94$  ppm;  $^{13}\text{C}$ :  $\delta=118.26$  ppm). The elemental analyses were performed by the scientific staff of TUM on a Flash EA 1112.

The electrochemical tests were performed with a Reference 600 Potentiostat ZRA controlled by the Gamry Framework software. All measurements were performed at room temperature and the used scan speed was 25 mV/s. The used electrodes were the glassy carbon ETO074 with 1 mm diameter as working electrode, Pt/titanium wire anode ETO074 as counter electrode and the Ag/AgCl as QRE.

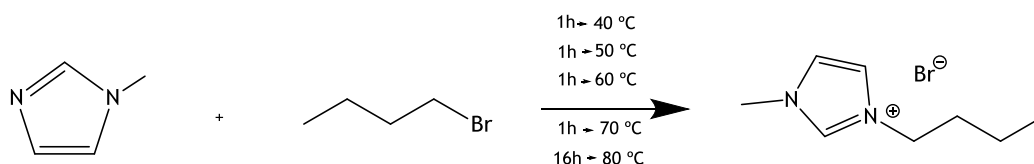
### 3.3 Procedure

The first step in the synthesis of the proposed ILs was the synthesis of the three bromide salts which would be precursors to the synthesis of the proposed ILs by anion substitution.

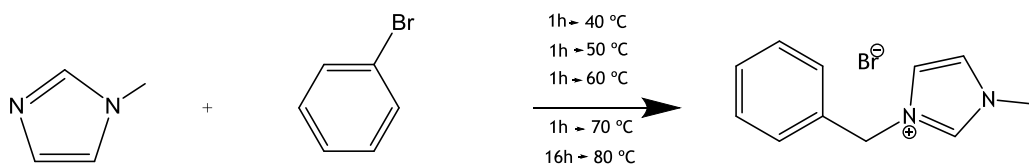
#### 3.3.1 Bromides synthesis

A scheme for the bromides reactions can be seen in Fig. 7.

Synthesis of 1-butyl-3-methylimidazoliumbromide [BMIm][Br]



Synthesis of 1-benzyl-3-methylimidazoliumbromide [BnMIm][Br]



Synthesis of 1-pentafluorobenzyl-3-methylimidazoliumbromide [Bn<sup>F</sup>MIm][Br]

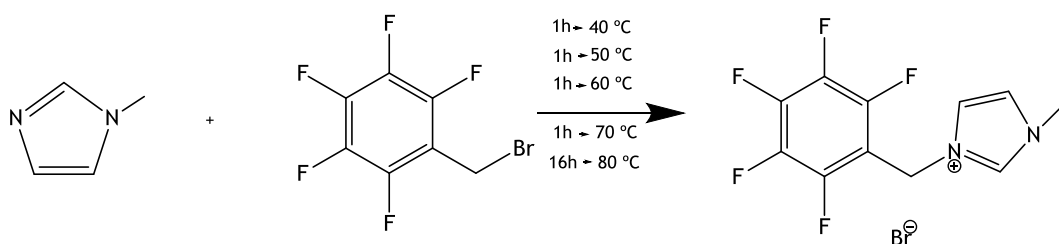


Figure 7. Scheme with the bromides reactions.

The syntheses were performed in 50 mmols batches. For each synthesis, 50 mmols of 1-methylimidazole (MIm) ( $C_4H_6N_2$ ) and 55 mmol of butyl bromide (BuBr) ( $C_4H_9Br$ ), benzyl bromide (BnBr) ( $C_6H_5Br$ ) and 2,3,4,5,6-pentafluorobenzyl bromide (<sup>F</sup>BnBr) ( $C_7H_2BrF_5$ ) were weighed. The respective weights are shown in the Tab. 3.

*Table 3. Weights of used reactants for the bromides synthesis*

Reactants	Weight(g)
MIm	4.10
BuBr	7.54
BnBr	9.40
<sup>F</sup> BnBr	14.34

50 mL of toluene ( $C_7H_8$ ) was used as solvent for the reactions which were done in 250 mL round flasks. The reactions proceeded at 40 °C, and were consecutively warmed at the rate of 10 °C per hour in an oil bath. After reaching the desired temperature of 80 °C, the reaction was left overnight under reflux conditions. In the end, two phases were present for all the synthesized bromides and the upper phase that only contained the solvent was decanted. The small amount of toluene left was removed for three hours in the rotary evaporator at 75 mbar and 40 °C.

For purification, the products were washed three times with 10 mL of diethyl ether ( $C_4H_{10}O$ ) in order to remove the excess reactant. Each of the washes was done for 10 minutes while stirring. The diethyl ether was then removed for one hour in the rotary evaporator at 850 mbar and 40 °C.

The [BMIm][Br] and the [<sup>F</sup>BnMIm][Br] crystalized as white and light yellow powders, respectively, while the [BnMIm][Br] was obtained as a very viscous light brown liquid. The [<sup>F</sup>BnMIm][Br] crystallization occurred in the rotary evaporator, the [BMIm][Br] crystalized in the fridge at 4 °C.

### 3.3.2 Anion Substitution

Seven ILs were successfully synthesized. They were the [BMIm][TFSI] ( $C_{10}H_{15}F_6N_2O_4S_2$ ), [BnMIm][TFSI] ( $C_{13}H_{13}F_6N_2O_4S_2$ ), [<sup>F</sup>BnMIm][TFSI] ( $C_{13}H_8F_{11}N_2O_4S_2$ ), [BMIm][PF<sub>6</sub>] ( $C_8H_{15}F_6N_2P$ ), [BnMIm][PF<sub>6</sub>] ( $C_{11}H_{13}F_6N_2P$ ), [<sup>F</sup>BnMIm][PF<sub>6</sub>] ( $C_{11}H_8F_{11}N_2P$ ) and [BnMIm][BF<sub>4</sub>] ( $C_{11}H_{13}BF_4N_2$ ).

The salts used for the anion substitutions were lithiumbis(trifluoromethanesulfonyl)imide (LiTFSI) ( $C_2F_6LiO_4S_2$ ), ammonium hexafluorophosphate (NH<sub>4</sub>PF<sub>6</sub>) and ammonium tetrafluoroborate (NH<sub>4</sub>BF<sub>4</sub>) whose anions are shown in Fig. 8.

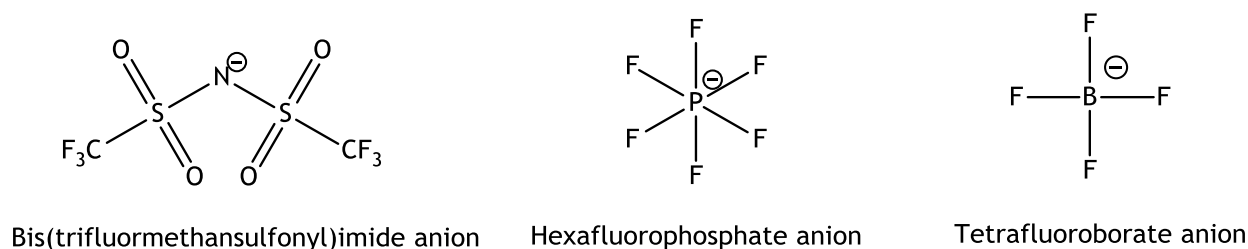


Figure 8. Anions of the salts used for the anions substitutions.

The substitutions of the bromide salts to TFSI, PF<sub>6</sub> and BF<sub>4</sub> salts were done in 30 mmol batches. For each substitution reaction, 30 mmol of each synthesized bromide IL, [BMIm][Br], [BnMIm][Br], [Bn<sup>F</sup>MIm][Br] and 36 mmols of each salt, LiTFSI, NH<sub>4</sub>PF<sub>6</sub>, NH<sub>4</sub>BF<sub>4</sub> were weighed. The respective weights are shown in Tab. 4.

Table 4. Weights of used reactants for the anions substitutions.

Reactants	Weight (g)
[BMIm][Br]	6.57
[BnMIm][Br]	7.59
[Bn <sup>F</sup> MIm][Br]	10.29
LiTFSI	10.35
NH <sub>4</sub> PF <sub>6</sub>	5.87
NH <sub>4</sub> BF <sub>4</sub>	3.77

For the anion substitution of bromide to the TFSI salts, the bromide was dissolved in 100 mL of water, while for the PF<sub>6</sub> and BF<sub>4</sub> salts only 20 mL of water was used as solvent. This was the method chosen since these ILs showed to be more soluble in water than the TFSI ILs and to use similar proportions to the ones used in the work of Laszlo and Compton [52]. The excess reactant was added slowly to the solution. The reactions were all stirred at room temperature for 16 hours in 250 mL Erlenmeyer flasks. In the end two phases were seen in all the solutions except for the [Bn<sup>F</sup>MIm][TFSI] and [Bn<sup>F</sup>MIm][PF<sub>6</sub>], which were milky foamed solutions dissolved in water. For the [BMIm][TFSI] and [BnMIm][TFSI] the water phase was decanted off while the organic phase was washed three times with 100 mL of water, to remove the excess of reactant salt present in the solution. Freshly distilled dichloromethane

(DCM) ( $\text{CH}_2\text{Cl}_2$ ) was added to dissolve the product and the water left on the ionic liquid was removed with the addition of a small amount of desiccant magnesium sulfate ( $\text{MgSO}_4$ ).

The mixture was stirred for 30 minutes and afterwards was filtered. The DCM was then removed for half an hour in the rotary evaporator at 750 mbar and 40°C. For the ILs with the  $[\text{Bn}^{\text{F}}\text{MIm}]$  cation, the water was extracted with vacuum filtration while the product was washed with sprayed water. As for the  $[\text{BMIm}][\text{PF}_6]$ ,  $[\text{BnMIm}][\text{PF}_6]$  and  $[\text{BnMIm}][\text{BF}_4]$  as the miscibility in water was considerable, the washing step was made with a volume ratio of 3 DCM to 1 of water. Afterwards the DCM was evaporated for half an hour in the rotary evaporator at 750 mbar and 40 °C, and the water at 55 mbar and 50 °C till no more bubbling was seen exiting the IL. In the Tab. 11 in the Annex 2 is summarized the final reaction appearance, the extraction method as well as the final product appearance for each synthesized IL.

Since it is known that the size of the EW is inversely proportional to the water content in the ionic liquids [40], all the products were transferred to Schlenk tubes, and dried over 16 hours under reduced pressure in the Schlenk line, at room temperature, in order to remove the vestigial water.

The purity of the ionic liquids was determined by  $^1\text{H}$  and  $^{13}\text{C}$  NMR spectroscopy, followed by elemental analysis. The first results of elemental analysis for the three TFSI salts revealed the presence of the bromide anion. The washing was repeated for these three salts plus three washes with diethyl ether. The ether was then removed for one hour in the rotary evaporator at 850 mbar and 40°C.

After this wash, it was attempted to do an extra cleaning with activated charcoal. This method has already been reported as successful in the removal of impurities from ILs [53]. However this treatment with adsorbents launched some controversy due to the possibility of adding extra impurities, even harder to extract [54]. Due to this possibility, only one third of the samples were subject to this method.

The samples were dissolved in DCM and 250 mg of activated charcoal was added to the solution and stirred for 2 hours at 30 °C. Afterwards the charcoal was filtered and the DCM removed in one hour in the rotary evaporator. One sample of each of the TFSI ILs with charcoal treatment and without were examined with elemental analysis for further comparison.

By observation the only difference noticed was in the  $[\text{Bn}^{\text{F}}\text{MIm}][\text{TFSI}]$  which previously had a light yellow colour, and after the charcoal purification turned into a white crystal. It has been already reported by Nockemann *et al.* that ILs tend to be contaminated by coloured impurities that can be removed by treatment with active charcoal [55].

### 3.3.3 Electrochemical tests

Since soluble oxygen is electrochemically active, its reduction can be a problem for accurate electrochemical window measurements [56]. To make sure that the electrochemical tests were carried out under inert atmosphere, all solutions for the LSV tests were prepared in a glove box operating with argon. Each of the IL solutions of 0.10 M and 0.25 M were prepared inside electrochemical cells with 1 mL of lithium hexafluorophosphate ( $\text{LiPF}_6$ ) as solvent. The respective weights are shown in the Tab. 5.

*Table 5. Weights for the LSV solutions*

Ionic Liquid	0.1 M (mg)	0.25 M (mg )
[BMIm][TFSI]	41.9	105.0
[BnMIm][TFSI]	45.3	113.0
[Bn <sup>F</sup> MIm][TFSI]	54.3	136.0
[BMIm][PF <sub>6</sub> ]	28.4	71.0
[BnMIm][PF <sub>6</sub> ]	31.8	79.5
[Bn <sup>F</sup> MIm][PF <sub>6</sub> ]	40.8	102.0
[BnMIm][BF <sub>4</sub> ]	26.0	65.0

Ideally the LSV tests should be done inside the glove box to make sure that no oxygen or water would enter in the solution, however in the present work that was not possible. The electrochemical cells were sealed with parafilm. The transportation from the glovebox to the LSV room was made with the samples inside a bigger flask also sealed with parafilm. The time between this moving was never more than 15 minutes.

Before each measurement a washing and polishing procedure was done to the electrodes. In the first trial of each sample, the three electrodes were washed with deionized water, methanol and acetone. Then a polishing step was done with diamond polisher followed by alumina polisher. Between trials only the WE and RE were cleaned, and this process was always as it follows: rinsed with water and acetone, polished in the diamond polisher, rinsed again, polished in alumina polisher and followed by a last wash. In the end the parafilm seal was pierced by the three electrodes and the tests began. Two trials were done for each sample. The data was inputted for the LSV tests as it is shown in Tab. 6.

*Table 6. Data inputted in Gamry framework software.*

<b>Initial potencial</b>	Between 4.5 and 3.5 V
<b>Final potencial</b>	Between -4.5 and -3.5 V
<b>Scan rate</b>	25 mV/s
<b>Step size</b>	1 mV
<b>Max current</b>	0.1 mA

## 4 Results and discussion

### 4.1 Products characterization

In all the displayed NMR results it is also presented the respective molecule. The lower case letters are always written first in the brackets and can also be seen in the molecules figures. They represent the correspondent  $^1\text{H}$  signals, while the numbers written after each peak signal represent the  $^{13}\text{C}$ . All the obtained spectrums are presented in the Annex 3.

#### 4.1.1 Bromides spectrums

Due to being intermediate products, the synthesized bromides were only characterized with  $^1\text{H}$  and  $^{13}\text{C}$  NMR spectrometry. It is only presented one graph for each synthesis, and they can be seen in the following Fig. 9 to 11.

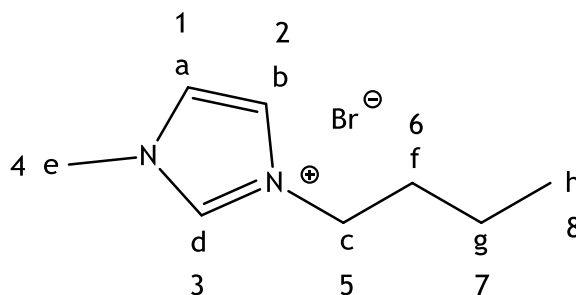


Figure 9. [BMIm][Br]

$^1\text{H}$  NMR (400MHz,  $\text{CDCl}_3$ , RT, ppm)  $\delta$  = 10.01 (d, 1H, s), 7.52 (b, 1H, s), 7.41 (a, 1H, s), 4.11 (c, 2H, t), 3.89 (e, 3H, s), 1.67 (f, 2H, quin), 1.15 (g, 2H, sex), 0.71 (h, 3H, t);

$^{13}\text{C}$  NMR (100.28 MHz,  $\text{CDCl}_3$ , RT, ppm)  $\delta$  = 136.53 (3), 123.53 (2), 121.91 (1), 49.29 (5), 36.23 (4), 31.70 (6), 18.95 (7), 13.02 (8).



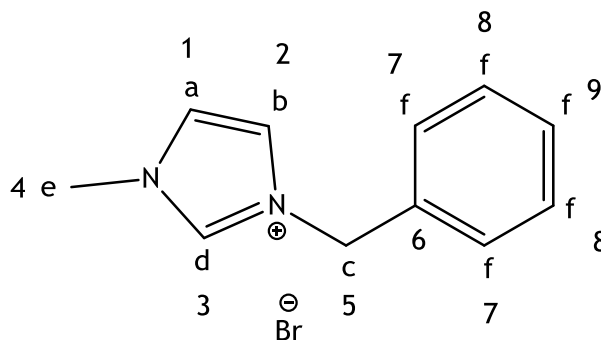
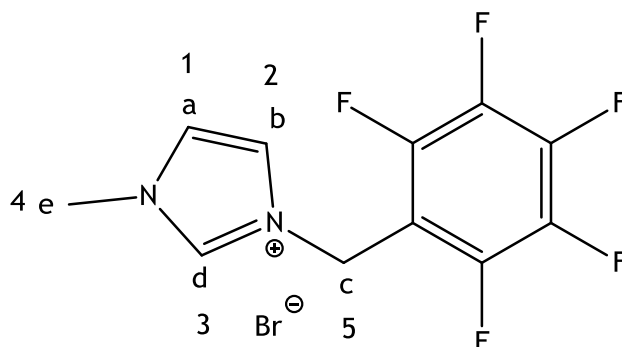


Figure 10. [BnMIm][Br]

$^1\text{H}$  NMR (400MHz,  $\text{CDCl}_3$ , RT, ppm)  $\delta$  = 10.22 (d, 1H, s), 7.63 (b, 1H, s), 7.51 (a, 1H, s), 7.44-7.25 (f, 5H, m), 5.53 (c, 2H, s), 3.96 (e, 3H, s);

$^{13}\text{C}$  NMR (100.28 MHz,  $\text{CDCl}_3$ , RT, ppm)  $\delta$  = 136.96 (3), 133.10 (6), 129.38 (7), 129.32 (8), 128.92 (9), 123.81 (2), 122.06 (1), 53.10 (5), 36.73 (4).

Figure 11. [Bn<sup>F</sup>MIm][Br]

$^1\text{H}$  NMR (400MHz,  $\text{CDCl}_3$ , RT, ppm)  $\delta$  = 10.37 (d, 1H, s), 7.70 (b, 1H, s), 7.57 (a, 1H, s), 5.80 (c, 2H, s), 4.09 (e, 3H, s);

$^{13}\text{C}$  NMR (100.28 MHz,  $\text{CDCl}_3$ , RT, ppm)  $\delta$  = 137.91 (3), 124.91 (2), 122.25 (1), 41.02 (5), 37.06 (4).

In this  $^{13}\text{C}$  NMR spectrum it is not possible to see the atom carbons of the  $^{\text{F}}\text{Bn}$  group, this is due to the fluorine atoms that tend to disturb the proper measuring of the carbon atoms. The excess of bromide reactant would be seen in the alkane region (1-2 ppm) and this was never noticed in the analysed spectrums.

#### 4.1.2 Final ILs characterization

The final ILs products were characterized with  $^1\text{H}$  and  $^{13}\text{C}$  NMR spectrometry and elemental analysis. It is only presented one graph for each synthesis, and they can be seen in the following Fig. 12 to 18. For the TFSI salts it is also shown the elemental analysis results for the samples cleaned with the active charcoal method (ACM).

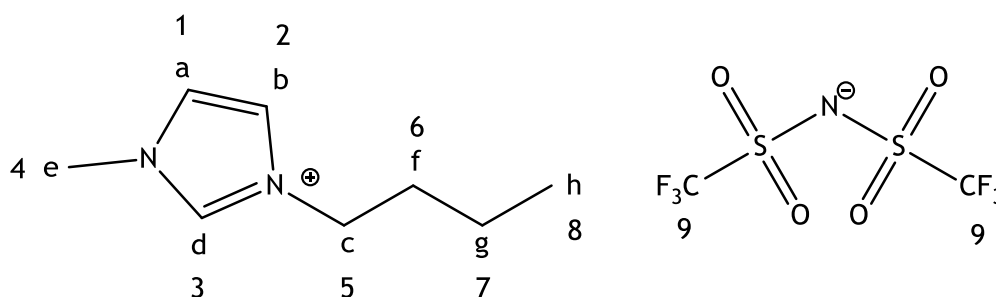


Figure 12. [BMIm][TFSI]

$^1\text{H}$  NMR (400MHz,  $\text{CDCl}_3$ , RT, ppm)  $\delta$  = 8.76 (d, 1H, s), 7.30 (b, 1H, s), 7.28 (a, 1H, s), 4.17 (c, 2H, t), 3.94 (e, 3H, s), 1.85 (f, 2H, quin), 1.35 (g, 2H, sex), 0.96 (h, 3H, t)

$^{13}\text{C}$  NMR (100.28 MHz,  $\text{CDCl}_3$ , RT, ppm)  $\delta$  = 136.17 (3), 123.80 (2), 122.37 (1), 121.51 (9), 118.32 (9), 50.07 (5), 36.44 (4); 32.04 (6); 19.45 (7); 13.32 (8)

Elemental analysis (%):

Calculated: C 28.64, H 3.61, N 10.0, S 15.29, O 15.26, F 27.18;

Found: C 28.31, H 3.82, N 9.82, S 14.97, O n.a, F 27.3.

Found ACM: C 28.41, H 3.91, N 9.88, S 15.06, O n.a, F 26.7.

A peak was seen at the 1.61 (1H, s) correspondent to the water in the solvent. A grease peak at 0.37 ppm was seen in this measurement, both of which will not be reported from now on [57]. The compound not washed with the charcoal method had slightly better results than the one where the extra clean was done. In this case the cleaning with charcoal had no advantage.

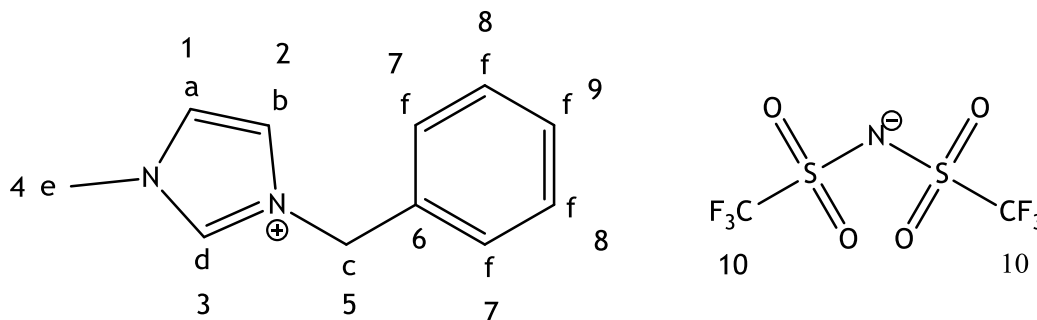


Figure 13. [BnMIm][TFSI].

$^1\text{H}$  NMR (400MHz,  $\text{CDCl}_3$ , RT, ppm)  $\delta$  = 8.78 (d, 1H, s), 7.42-7.34 (f, 5H, M), 7.28 (b, 1H, s), 7.19 (a, 1H, s), 5.30 (c, 2H, s), 3.91 (e, 3H, s)

$^{13}\text{C}$  NMR (100.28 MHz,  $\text{CDCl}_3$ , RT, ppm)  $\delta$  = 136.22 (3), 132.33 (6), 129.93 (7), 129.74 (8), 129.01 (9), 123.91 (2), 122.22 (1), 121.52 (10), 118.33 (10), 53.76 (5), 36.55 (4), 31.07

Elemental analysis (%):

Calculated: C 34.44, H 2.89, N 9.27, S 14.14, O 14.12, F 25.14;

Found: C 34.11, H 2.98, N 9.11, S 14.05, O n.a, F 26.20.

Found acm: C 34.65, H 2.88, N 8.76, S 14.41, O n.a, F 25.7.

A peak was seen in 31.07 (1H, s) correspondent to acetone [57]. Some traces of acetone from the tubes cleaning process was probably present in the NMR tubes. The fluorine value found in the elemental analysis is 1.1 % above the calculated and this is likely due to some reactant that was not removed during the washing process.

The ACM percentage of F was found 0.56 % above the calculated value. Although this value is also above the 0.4 % error of the elemental analysis it is 0.54 % below the found value for the sample not cleaned with the active charcoal method. It is possible to conclude that the cleaning with the charcoal had some effect in the removal of the F impurities present in the IL.

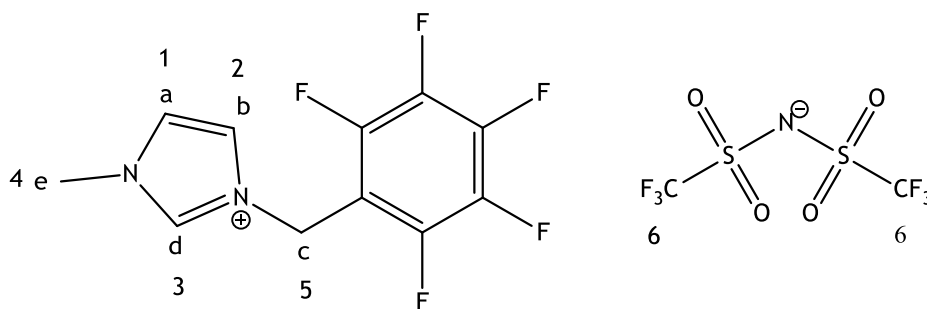


Figure 14.  $[Bn^F MIm][TFSI]$ .

$^1H$  NMR (400MHz,  $CD_3CN$ , RT, ppm)  $\delta$  = 8.52 (d, 1H, s), 7.39 (b, 1H, s), 7.36 (a, 1H, s), 5.44 (c, 2H, s), 3.81 (e, 3H, s).

$^{13}C$  NMR (100.28 MHz,  $CD_3CN$ , RT, ppm)  $\delta$  = 137.53 (3), 125.06 (2), 123.37 (1), 41.14 (5), 37.01 (4).

Elemental analysis (%):

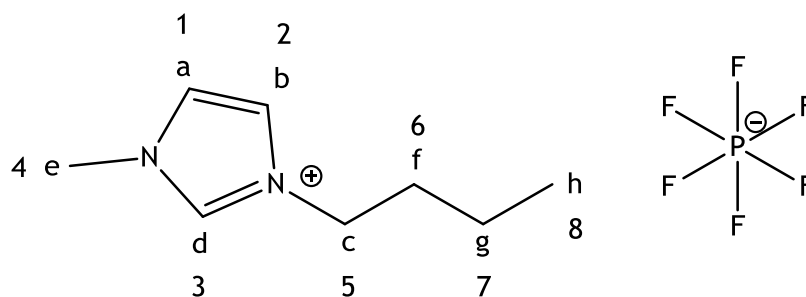
Calculated: C 28.74, H 1.48, N 7.73, S 11.80, O 11.78, F 38.46;

Found: C 28.71, H 1.45, N 7.65, S 12.53, O n.a, F 39.70.

Found cm: C 28.69, H 1.40, N 7.73, S 11.73, O n.a, F 39.2.

In the  $^1H$  NMR at 5.44 ppm is possible to see that the integral is slightly higher than 2, that is due to the presence of DCM [57]. This was neglected due to the high volatility of the impurity and because the ILs would be dried again in the Shlenk line. In the elemental analysis results it is possible to see that no DCM is left in the product.

The F value is 1.24 % higher than the calculated value for the normally cleaned sample while the charcoal method percentage of fluorine was found 0.74 % above the calculated. The same conclusions as for the last IL can be made.

Figure 15. [BMIm][PF<sub>6</sub>].

<sup>1</sup>H NMR (400MHz, DMSO-d<sub>6</sub>, RT, ppm)  $\delta$  = 9.00 (d, 1H, s), 7.69 (b, 1H, s), 7.62 (a, 1H, s), 4.13 (c, 2H, t), 3.82 (e, 3H, s), 1.74 (f, 2H, quin), 1.25 (g, 2H, sex), 0.85 (h, 3H, t).

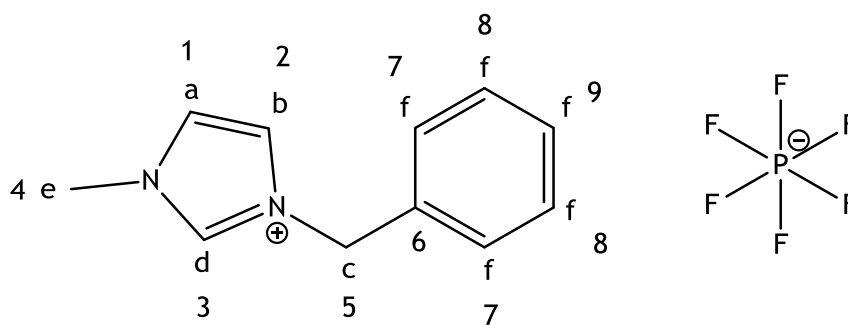
<sup>13</sup>C NMR (100.28 MHz, DMSO-d<sub>6</sub>, RT, ppm)  $\delta$  = 136.62 (3); 123.85 (2); 122.51 (1); 48.89 (5); 36.00 (4); 31.61 (6); 19.06 (7); 13.53 (8).

Elemental analysis (%):

Calculated: C 33.81, H 5.32, N 9.86, P 10.90, F 40.11;

Found: C 33.50, H 5.32, N 9.70, P 10.61, F 40.70.

The F found is 0.59 % above the calculated value.

Figure 16. [BnMIm][PF<sub>6</sub>].

<sup>1</sup>H NMR (400MHz, DMSO-d<sub>6</sub>, RT, ppm)  $\delta$  = 9.13 (d, 1H, s), 7.72 (b, 1H, s), 7.65 (a, 1H, s), 7.42-7.39 (f, 5H, m), 5.33 (c, 2H, s), 3.83 (e, 3H, s).

<sup>13</sup>C NMR (100.28 MHz, DMSO-d<sub>6</sub>, RT, ppm)  $\delta$  = 136.80 (3), 134.96 (6), 129.36 (7), 129.15 (8), 128.57 (9), 124.28 (2), 122.57 (1), 52.24 (5), 36.15 (4).

Elemental analysis (%):

*Calculated:* C 41.52, H 4.12, N 8.80, P 9.73, F 35.82;

*Found:* C 41.18, H 4.18, N 8.69, P 9.26, F 35.4.

The P and F value are respectively 0.47% and 0.42%, below the calculated.

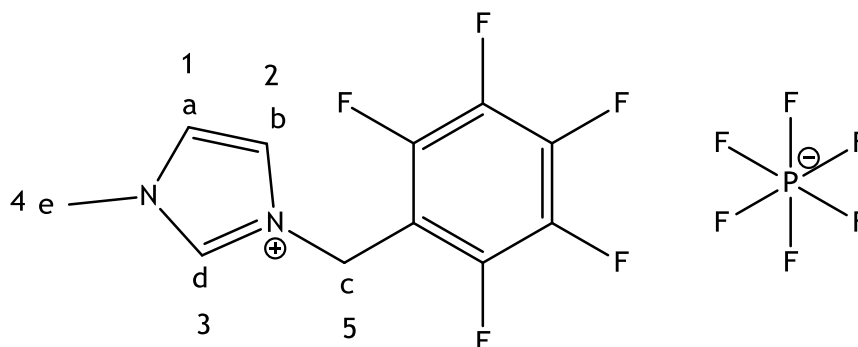


Figure 17.  $[Bn^F MIm][PF_6]$

$^1H$  NMR (400MHz,  $CD_3CN$ , RT, ppm)  $\delta$  = 8.51(d, 1H, s), 7.40(b, 1H, s), 7.36(a, 1H, s), 5.46( c, 2.17H, t), 3.81 (e, 3.22H, s).

$^{13}C$  NMR (100.28 MHz,  $CD_3CN$ , RT, ppm)  $\delta$  = 137.49 (3); 125.05 (2); 123.37 (1); 41.13 (5); 37.00 (4).

Elemental analysis (%):

*Calculated:* C 32.37, H 1.98, N 6.86, P 7.59, F 51.20;

*Found:* C 32.38, H 2.68, N 6.80, P 7.91, F 50.7.

The higher integral value at 5.46 ppm is probably due to the presence of some DCM that was still inside the IL. The H value was found to be 0.7 % higher than the calculated probably due to the presence of water in the IL. The product was dried again in the Shlenk line.

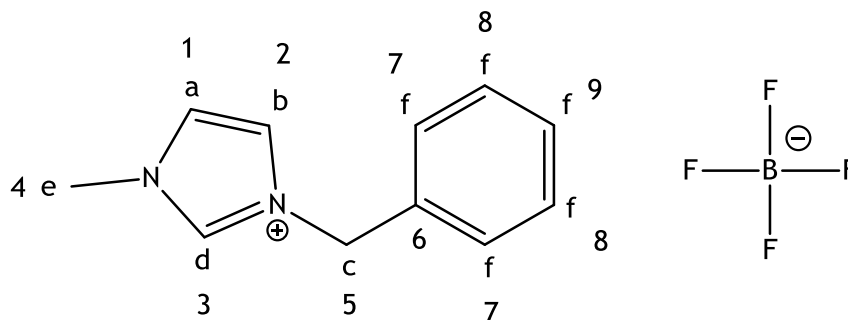


Figure 18. [BnMIm][BF<sub>4</sub>].

<sup>1</sup>H NMR (400MHz, DMSO-d<sub>6</sub>, RT, ppm)  $\delta$  = 9.11 (d, 1H, s), 7.71 (b, 1H, s), 7.64 (a, 1H, s), 7.46-7.33(f, 5H, m), 5.37 (c, 2H, s), 3.82 (e, 3H, s).

<sup>13</sup>C NMR (100.28 MHz, DMSO-d<sub>6</sub>, RT, ppm)  $\delta$  = 136.79 (3); 134.96 (6); 129.38 (7); 129.17 (8); 128.59 (9); 124.29 (2); 122.58 (1); 52.26 (5); 36.16 (4).

Elemental analysis (%):

Calculated: C 50.81, H 5.04, N 10.77, B 4.16, F 29.22;

Found: C 50.87, H 5.25, N 10.68, B n.a, F 28.82.

Two ionic liquids were found having high purity, the [BMIm][TFSI] and [BnMIm][BF<sub>4</sub>].

## 4.2 Electrochemical tests results

In the Fig. 19 and 20 it is shown the graphs as they were plotted by the software Gamry Framework.

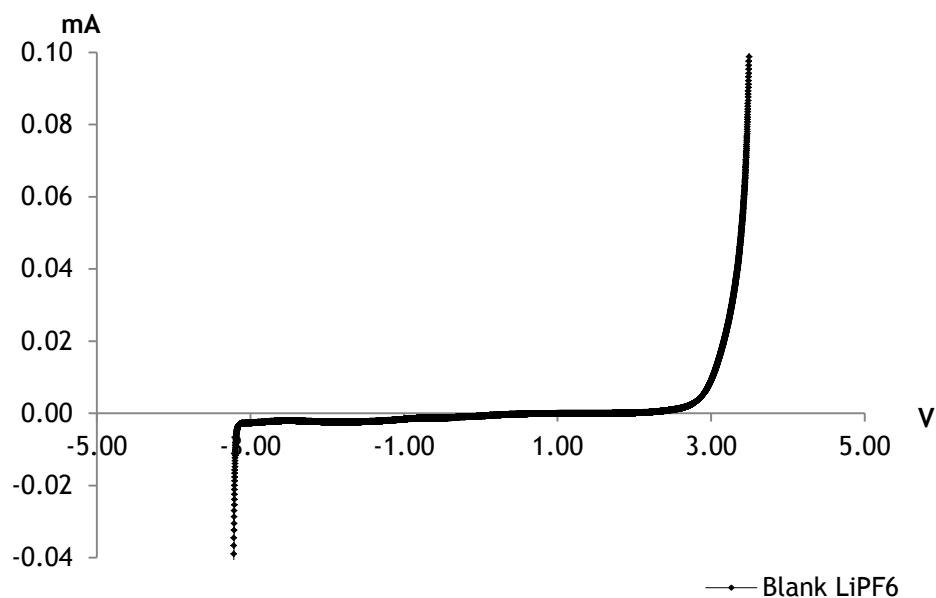


Figure 19. LSV graph of Blank LiPF<sub>6</sub>.

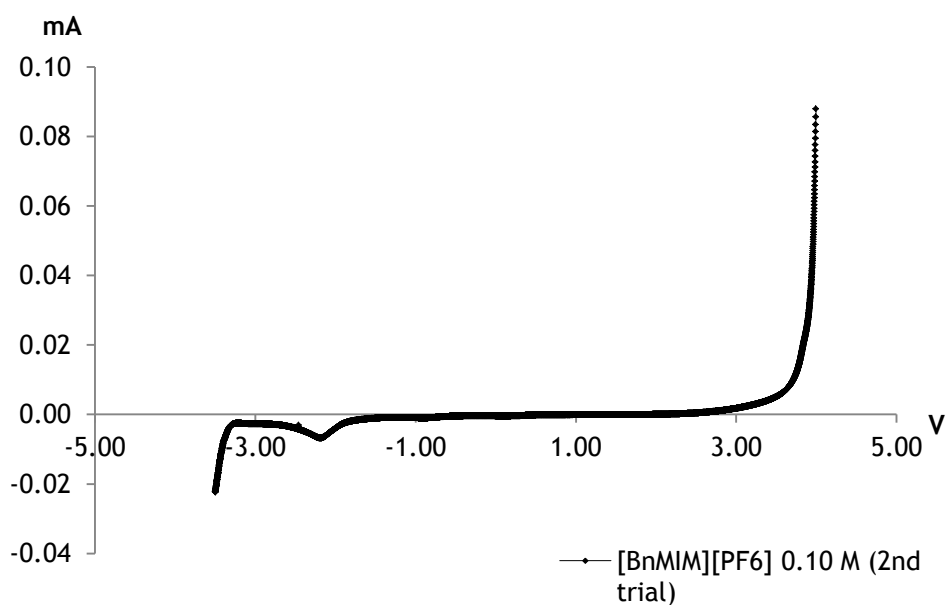


Figure 20. LSV graph of [BnMIM][PF<sub>6</sub>] 0.10 M (2nd trial).



It is possible to notice the slope present around -2 V for the IL and in slight extension, the blank sample. This slope was present in all the ionic liquids, in greater or lesser extent. However, for the ILs the slopes have always similar proportions to the one in the presented in the Fig. 20.

It is important to notice that even with all the efforts made to try to get an inert atmosphere inside the vial, it is impossible to assure that at the moment of the piercing of the seal some air and humidity from the air did not enter. Silvester and Compton showed that the EWs for imidazolium-based ILs suffer a narrowing in the cathodic area when performed in ambient air [58]. This bigger affinity of imidazolium with water than other moieties can be a reason for the bigger slopes in all the tested ILs. In the work of Hayyan *et al.* the small slope is also seen in some of the electrochemically tested ILs, the authors relate the issue with the amount of impurities present in the ILs [40, 59]. However in the present work two ILs were synthesized with higher purity than the others, the [BMIm][TFSI] and the [BnMIm][BF<sub>4</sub>], by observing their graphs and comparing with one of the less pure ILs, the [Bn<sup>F</sup>MIm][TFSI] it is not possible to conclude the same. This comparison can be seen in the Fig. 43 in the Annex 4. This comparison is not the more accurate possible since the compared ionic liquids are different and their interaction with the impurities may be different.

After normalizing the y axis with regard to the working electrode area (0.007854 cm<sup>2</sup>), the graphs showed in Fig. 19 and 20 were obtained as it showed in the Fig. 21.

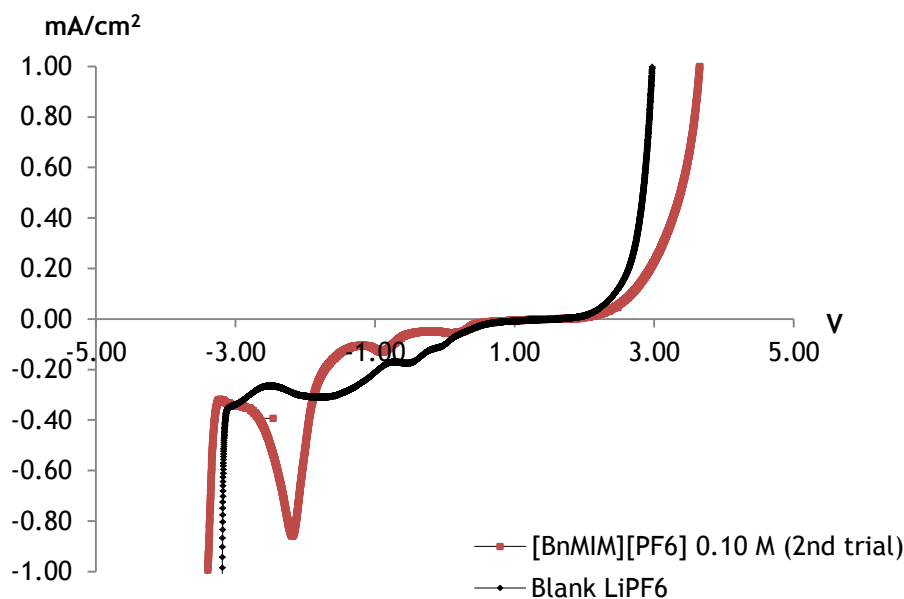


Figure 21. LSV graph of [BnMIM][PF<sub>6</sub>] 0.1 M (2nd trial) and Blank LiPF<sub>6</sub>.

With current density ( $\text{mA}/\text{cm}^2$ ) in the y axis the slope produces a bigger impact in the graph. This way in order to be possible to see the full EW and be able to compare the obtained EWs of the different ILs it was chosen to calculate the EWs with the maximum cut-off current density advisable,  $1 \text{ mA}/\text{cm}^2$  [40].

The CL, AL and EWs obtained for each performed test are shown in Tab. 7.

Table 7. LSV EWs results

Ionic Liquid	EWs	
	1 <sup>st</sup> trial	2 <sup>nd</sup> trial
Blank	6.17	6.16
[BMIm][TFSI] 0.1 M	6.10	6.07
[BMIm][TFSI] 0.25 M	<del>4.72</del>	6.23
[BnMIm][TFSI] 0.1 M	6.05	6.23
[BnMIm][TFSI] 0.25 M	6.18	<del>4.22</del>
[Bn <sup>F</sup> MIm][TFSI] 0.1 M	6.34	6.43
[Bn <sup>F</sup> MIm][TFSI] 0.25 M	6.26	6.26
[BMIm][PF <sub>6</sub> ] 0.1 M	6.07	6.10
[BMIm][PF <sub>6</sub> ] 0.25 M	5.89	6.15
[BnMIm][PF <sub>6</sub> ] 0.10 M	6.25	7.05
[BnMIm][PF <sub>6</sub> ] 0.25 M	6.31	6.10
[Bn <sup>F</sup> MIm][PF <sub>6</sub> ] 0.10 M	6.39	6.50
[Bn <sup>F</sup> MIm][PF <sub>6</sub> ] 0.25 M	6.27	6.50
[BnMIm][BF <sub>4</sub> ] 0.10 M	6.30	6.33
[BnMIm][BF <sub>4</sub> ] 0.25 M	6.37	6.53

The EWs present in the Tab. 7 cannot be compared with data from literature for the following reasons; literature was not found reporting EWs with the same electrodes for any of

these ILs and it was not possible to ensure totally inert air conditions. The presented ILs EWs are only comparable with the ones present in this thesis. The CL and AL values present in the Tab. 12 in the Annex 4 cannot be compared with others present in literature for the reasons stated above and because no internal reference compound, like ferrocene, was used to calibrate the measurements. However some trends are analysed in this chapter.

The obtained EWs with values below 5 V are crossed out in Tab. 7 and have been discarded from the following analysis. The great voltage difference between the two trials with each ionic liquid and also between the different ILs showed in Tab. 7 caused the discard of the values outside the general pattern. It is thought that in these measurements a problem must have happened, probably an inadequate cleaning step.

#### 4.2.1 EW overview

The wider obtained EW was 7.05 V, obtained for the [BnMIm][PF<sub>6</sub>] 0.10 M, while the narrower EW found was 5.89 for the [BMIm][PF<sub>6</sub>].

Comparing with the work of Can-can *et al*, it is possible to see that the value of the [BMIm][PF<sub>6</sub>] has been reported with a wider EW than the one for [BMIm][TFSI] with experiments done with the same electrodes. The same happened in this work. Comparing the averages obtained for some groups of ILs it is possible to realize some patterns. In Tab. 8 are reported the averages for the group of EWs with the same cation and same concentration.

Table 8. Average values for the same cation and concentration

Cation \ Concentration	Concentration	
	0.1 M	0.25 M
[BMIm] <sup>+</sup>	6.09 V	6.09 V
[BnMIm] <sup>+</sup>	6.36 V	6.30 V
[Bn <sup>F</sup> MIm] <sup>+</sup>	6.42 V	6.32 V

It is possible to establish the following order for the cations EWs for both concentrations: [BMIm]<sup>+</sup> < [BnMIm]<sup>+</sup> < [Bn<sup>F</sup>MIm]<sup>+</sup>. It is also possible to see that apart from the BMIm cation the EW tends to get narrower for the higher concentrations. For the anions, the analysis has to be done with respect only to the BnMIm cations since it is the only cation

coupled with the three anions. In Tab. 9 are reported the averages for the group of EWs with the  $[\text{BnMIm}]^+$  the same anion and same concentration.

Table 9. Average values for BnMim cation, same anion and concentration.

Concentration Anion	0.1 M	0.25 M
$[\text{TFSI}]^-$	6.14 V	6.20 V
$[\text{PF}_6]^-$	6.65 V	6.20 V
$[\text{BF}_4]^-$	6.32 V	6.45V

The best result of this thesis was obtained for the  $[\text{BnMIm}][\text{PF}_6]$ , for lower concentrations. In this scenario, the  $[\text{PF}_6]$  was the anion with the best performance. For 0.1 M the order in width for the EW is as follows:  $[\text{PF}_6]^+ > [\text{BF}_4]^+ > [\text{TFSI}]^+$ .

Although the results compiled in the work of Can-can *et al.* are for the  $[\text{BMIm}]$ , the order of the values discovered in Tab. 1 is the same as in this study. And it is also in accord with the performed work of Ue *et al.* [60]

In Tab. 10 the averages for the group of EWs with the same cation and same concentration are showed.

Table 10. Average values for the same anion and concentration

Concentration Anion	0.1 M	0.25 M
$[\text{TFSI}]^-$	6.20 V	6.23 V
$[\text{PF}_6]^-$	6.39 V	6.20 V

A more complete anion analysis can be done between the  $\text{PF}_6$  and TFSI since they have been synthesised coupled with the three cations. With this analysis it is possible to see that their performance is similar for 0.25 M but the  $\text{PF}_6$  has better results for 0.1 M. This decrease in the performance for higher concentrations can be explained by the much higher viscosities of the  $\text{PF}_6$  based ILs compared with the TFSI based ILs [61]. Observing the values regarding the same concentrations in the last three tables it is possible to see that sometimes the EW widens with an increase in the concentration and sometimes it narrows. With a more

attentive look it is possible to notice that the drop or increase is somehow related with the content of fluorine. ILs with more fluorine tend to have a decrease in their EW for the 0.25 molar solutions.

Another fact to note is that the bad measurements crossed out in Tab. 7 happened in the CL of TFSI ILs as can be seen in the Tab.12 seen in Annex 4. Besides the possibility of a bad washing step, this occurrence can be due to the lower hydrophobicity of the TFSI anion when compared with the  $\text{BF}_4$  and  $\text{PF}_6$ . Since these measurements were done under uncontrolled atmosphere conditions it could happen that the TFSI ILs had a bigger interaction with the  $\text{H}_2\text{O}$  present in the air affecting the LSV measurement [48]. The fact that this also happened for the higher concentrations of this salt is another event that corroborates this idea.

## 5 Conclusions

Seven ILs were successfully synthesized and purified, two of them with high purity levels. Their electrochemical windows were characterized making it possible to establish the following relations to their width:  $\text{Bn}^{\text{F}}\text{MIm}^+ > \text{BnMIm}^+ > \text{BMIm}$ . A sequence was also established for the anions  $\text{PF}_6^- > \text{BF}_4^- > \text{TFSI}^-$  which is in accord to what was found in literature. Both  $[\text{BMIm}][\text{BF}_4]$  and  $[\text{Bn}^{\text{F}}\text{MIm}][\text{BF}_4]$  were synthesized, but their purification was not completed in the present work. The method used to order the referred sequences was based in a statistical approach done with the results. The failure of two EW characterizations caused that they only had one measurement reported as opposed to every other IL, who had two for each concentration. This fact, along with the absence of the  $[\text{BMIm}][\text{BF}_4]$  and  $[\text{Bn}^{\text{F}}\text{MIm}][\text{BF}_4]$  ILs from the electrochemical tests, makes the calculation of the average values a less rigorous approach, seen as the same number of events were not utilized for all the used anion and cation combinations. However, since the characterized EWs followed clear patterns, it is possible to assume that the obtained results were a success in identifying the most promising ILs in the scope of this work. It is possible to create a relation between the ions with better performances and the higher number of fluorine atoms in the molecule. Nonetheless, if someday it is applied, it is necessary to keep in mind that ILs with the  $\text{PF}_6^-$  and  $\text{BF}_4^-$  anions at certain temperatures are hydrolytically unstable and can evolve into HF [62, 63]. The inert air conditions necessary to benefit from their physical properties is another drawback shared by all the ILs synthesized in this work. The high prices of industrial scale inert air can be a prohibitive factor for some industries.

The EW values obtained are too wide when comparing with the available literature, this happened because of the maximum cut off current used which was  $1 \text{ mA/cm}^2$ . Most of the reported literature uses  $0.1 \text{ mA/cm}^2$ , however this needs to be adapted for each case.

However the sequences made make possible to predict which compounds should be studied more deeply in the future. Beyond the scope of the proposed work was also studied the effect of the charcoal on the purification of ILs, and this method had positive results in two out of three tested cases.

The work presented in this thesis was the beginning of a new topic in TUM, and it will be directly continued by a member of the research team. The ILs electrochemical tests should be reproduced with an internal reference, in order obtain reliable Cl and Al values, if possible ensuring inert atmosphere conditions. The ILs for which was not achieved an ideal

level of purity should be washed again. It would also be advisable to determine the water content of each ionic liquid before the new tests. Afterwards other important physical and chemical properties of the ILs should be tested e.g. viscosity, conductivity. Then it should be studied how the proposed ILs influence the lithium ion transport and the electrode interactions that occur in an operating lithium cell [34].

The biggest difficulties in the accomplishment of this thesis were at level of the purification of the ILs which was much time consuming. The work in a glove box was also a big challenge, namely in the accurate weighing of the ILs to make the solutions for the electrochemical tests. All the machinery inside the glove box room increased the room temperature, making it very hot and a more difficult task.

The ILs can turn to be the future of a wide range of applications, to expedite the research in this area some conventions should be made regarding the experimental conditions. The optimal electrodes combinations should be established in way that the CLs and ALs can be recorded with the same conditions. This would enable more accurate comparisons between different studies and consequently a better understanding of the chemical interactions at stake.

## References

1. Buchmann, I., *Batteries in a Portable World: A Handbook on Rechargeable Batteries for Non-Engineers*. Cadex Electronics Inc, 2011.
2. Fitzpatrick-Matthews, K. *The 'batteries of Babylon'*. 2009. Retrieved at [28/04/2015]; Available from: <http://www.badarchaeology.com/out-of-place-artefacts/anomalously-old-technology/the-%E2%80%98batteries-of-babylon%E2%80%99/>.
3. Volta, A. J. Banks, I. *On the electricity excited by the mere contact of conducting substances of different kinds*. Philosophical Magazine Series 1. **7**(28): p. 289-311, 1800
4. Kenyon, T.K., *Science and Celebrity: Humphry Davy's Rising Star*, in *Chemical Heritage Magazine*, Chemical Heritage Foundation, 2008
5. Coutts, A., *William Cruickshank of Woolwich*. Annals of Science, **15**(2): p. 121-133, 1959.
6. Kurzweil, P., *Gaston Planté and his invention of the lead-acid battery—The genesis of the first practical rechargeable battery*. Journal of Power Sources, **195**(14): p. 4424-4434, 2010.
7. Pilatowicz, G., Budde-Meiwes, H., Schulte, D., Kowal, J., Zhang, Y., Du, X., Salman, M., Gonzales, D., Alden, J., Sauer, D.U., *Simulation of SLI Lead-Acid Batteries for SOC, Aging and Cranking Capability Prediction in Automotive Applications*. Meeting Abstracts, **MA2011-02**(14): p. 706, 2011.
8. Whittingham, M.S., *Electrical Energy Storage and Intercalation Chemistry*. Science, **192**(4244): p. 1126-1127, 1976.
9. Besenhard, J.O., Fritz, H.P., *Cathodic reduction of graphite in organic solutions of alkali and NR<sub>4</sub><sup>+</sup> salts*. Journal of Electroanalytical Chemistry and Interfacial Electrochemistry, **53**(2): p. 329-333, 1974.
10. Schöllhorn, R., Kuhlmann, R., Besenhard, J.O., *Topotactic redox reactions and ion exchange of layered MoO<sub>3</sub> bronzes*. Materials Research Bulletin, **11**(1): p. 83-90, 1976.
11. Besenhard, J.O., Eichinger, J.O., *High energy density lithium cells: Part I. Electrolytes and anodes*. Journal of Electroanalytical Chemistry and Interfacial Electrochemistry, **68**(1): p. 1-18, 1976.
12. Eichinger, G., Besenhard, J.O., *High energy density lithium cells: Part II. Cathodes and complete cells*. Journal of Electroanalytical Chemistry and Interfacial Electrochemistry, **72**(1): p. 1-31, 1976.
13. Yoshino, A., *The Birth of the Lithium-Ion Battery*. Angewandte Chemie International Edition, **51**(24): p. 5798-5800, 2012.
14. Eshetu, G., Armand, M., Scrosati, B., Passerini, S., *Energy Storage Materials Synthesized from Ionic Liquids*. Angewandte Chemie International Edition, **53**(49): p. 13342-13359, 2014.
15. *What is a battery?* Retrieved at [30/04/2015]; Available from: <http://batt.lbl.gov/what-is-a-battery/>.
16. Bates, M., *HOW DOES A BATTERY WORK?* Ask an engineer 2012. Retrieved at [30/04/2015]; Available from: <http://engineering.mit.edu/ask/how-does-battery-work>.
17. Elsevier. *Reaxys*. Retrieved at [02/04/2015]; Available from: <https://www.reaxys.com/reaxys/secured/search.do>.



18. Angell, A.C., Ansari, Y., Zhao, Z., *Ionic Liquids: Past, present and future*. Faraday Discussions, **154**(0): p. 9-27, 2012.
19. Wilkes, J.S., *A short history of ionic liquids-from molten salts to neoteric solvents*. Green Chemistry, **4**(2): p. 73-80, 2002.
20. Gale, R.J., Gilbert, B., Osteryoung, R.A., *Raman spectra of molten aluminum chloride: 1-butylpyridinium chloride systems at ambient temperatures*. Inorganic Chemistry, **17**(10): p. 2728-2729, 2002.
21. Zaworotko, M.J., Wilkes, J.S., *Air and water stable 1-ethyl-3-methylimidazolium based ionic liquids*. Journal of the Chemical Society, Chemical Communications, (13): p. 965-967, 1992.
22. Bonhôte, P., Dias, A.P., Papageorgiou, N., Kalyanasundaram, K., Grätzel, M., *Hydrophobic, Highly Conductive Ambient-Temperature Molten Salts*. Inorganic Chemistry, **35**(5): p. 1168-1178, 1996.
23. Freemantle, M., *An Introduction to Ionic Liquids*. RSC Publishing, 2009.
24. Moreno, J.S., Jeremias, S., Moretti, A., Panero, S., Passerini, S., Scrosati, B., Appetecchi, *Ionic liquid mixtures with tunable physicochemical properties*. Electrochimica Acta, **151**(0): p. 599-608, 2015.
25. Berthod, A., Ruiz-Ángel, M.J., Carda-Broch, S., *Ionic liquids in separation techniques*. Journal of Chromatography A, **1184**(1-2): p. 6-18, 2008.
26. Somers, A. E., Howlett, P.C., MacFarlane, D.R., Forsyth, M., *A Review of Ionic Liquid Lubricants*. Lubricants, **1**(1): p. 3, 2013.
27. John, D.H., Reichert, W.M., Reddy, R.G., Rogers, R.D., *Heat Capacities of Ionic Liquids and Their Applications as Thermal Fluids*, in *Ionic Liquids as Green Solvents*, American Chemical Society. p. 121-133, 2003.
28. Ho, T.D., Zhang, C., Hantao, L.W., Anderson, J.L., *Ionic Liquids in Analytical Chemistry: Fundamentals, Advances, and Perspectives*. Analytical Chemistry, **86**(1): p. 262-285, 2014.
29. Olivier-Bourbigou, H., Magna, L., Morvan, D., *Ionic liquids and catalysis: Recent progress from knowledge to applications*. Applied Catalysis A: General **373**(1-2): p. 1-56, 2010.
30. Pham, T.P.T., Cho, C.W., Yun, Y.S., *Environmental fate and toxicity of ionic liquids: A review*. Water Research, **44**(2): p. 352-372, 2010.
31. Ohno, H., Yoshizawa, M., Mizumo, T., *Ionic Conductivity*, in *Electrochemical Aspects of Ionic Liquids*. John Wiley & Sons, Inc. p. 75-81, 2005.
32. Kim, J.K., Matic, A., Ahn, J.H., Jacobsson, P. *An imidazolium based ionic liquid electrolyte for lithium batteries*. Journal of Power Sources, **195**(22): p. 7639-7643, 2010.
33. Guerfi, A., Dontigny, M., Charest, P., Petitclerc, M., Lagacé M., Vijh, A., Zaghib, K. *Improved electrolytes for Li-ion batteries: Mixtures of ionic liquid and organic electrolyte with enhanced safety and electrochemical performance*. Journal of Power Sources, **195**(3): p. 845-852, 2010.
34. MacFarlane, D.R., Tachikawa, N., Forsyth, M., Pringle, J.M., *Energy applications of ionic liquids*. Energy and Environmental Science, **7**(1): p. 232-250, 2014.
35. Granqvist, C.G., *Handbook of Inorganic Electrochromic Materials*. Elsevier Science, 1995

36. Grande, L., Zamory, J., Koch, S.L., Kalhoff, J., Paillard, E., Passerini, S., *Homogeneous Lithium Electrodeposition with Pyrrolidinium-Based Ionic Liquid Electrolytes*. ACS Applied Materials & Interfaces, **7**(10): p. 5950-5958, 2015.
37. Liu, Y.S., Pan, G.B., *Ionic Liquids for the Future Electrochemical Applications*, in *Ionic Liquids: Applications and Perspectives*, A. Kokorin, Intech, p. 627-642, 2011.
38. Wei, S., Dandan, W., Ruifang, W., Kui, J., *Direct electrochemistry and electrocatalysis of hemoglobin in sodium alginate film on a BMIMPF<sub>6</sub> modified carbon paste electrode*. Electrochemistry Communications, **9**(5): p. 1159-1164, 2007.
39. Van Aken, K.L., Beidaghi, M., Gogotsi, Y., *Formulation of ionic-liquid electrolyte to expand the voltage window of supercapacitors*. Angew Chem Int Ed Engl, **54**(16): p. 4806-9, 2015.
40. Hayyan, M., Mjalli, F.S., Hashim, M.A., AlNashef, I.M., Mei, T.X., *Investigating the electrochemical windows of ionic liquids*. Journal of Industrial and Engineering Chemistry, **19**(1): p. 106-112, 2013.
41. Ong, S.P., Andreussi, O., Wu, Y., Marzari, N., Gerbrand, C., *Electrochemical Windows of Room-Temperature Ionic Liquids from Molecular Dynamics and Density Functional Theory Calculations*. Chemistry of Materials, **23**(11): p. 2979-2986, 2011.
42. Rogers, E.I., Šljukić, B., Hardacre, C., Compton, R.G., *Electrochemistry in Room-Temperature Ionic Liquids: Potential Windows at Mercury Electrodes*. Journal of Chemical & Engineering Data, **54**(7): p. 2049-2053. 2009.
43. Bard, A.L., Faulkner, L.R., *Electrochemical Methods: Fundamentals and Applications*. 2nd ed. New York: Wiley, 2001.
44. Robinson, J.W., Frame, E.S., Frame, G.M.II., *Undergraduate Instrumental Analysis*. 7th ed, New York: CRC Press, 2014.
45. Betz, D.H., *Olefin epoxidation with transition-metal catalysts in ionic liquids*, in *Inorganic chemistry*. Technische Universität München, 2011.
46. Can-can, Q., Yi-xin, H., Cun-Ying, X., Jian, L., Qi-bo, Z., Yan, L., *Research advances in electrochemical window of ionic liquids*. Guocheng Gongcheng Xuebao The Chinese Journal of Process Engineering, **14**(4): p. 694-707, 2014.
47. Zhao, C., Burrell G., Torriero, A.J., Separovic, F., Dunlop, N.F., MacFarlane, D.R., Bond, Alan M., *Electrochemistry of Room Temperature Protic Ionic Liquids*. The Journal of Physical Chemistry B, **112**(23): p. 6923-6936, 2008.
48. O'Mahony, A.M., Silvester, D.S., Aldous, L., Hardacre C., Compton R.G., *Effect of Water on the Electrochemical Window and Potential Limits of Room-Temperature Ionic Liquids*. Journal of Chemical & Engineering Data, **53**(12): p. 2884-2891, 2008.
49. Suarez, P.A.Z., Selbach, V.M., Dullius J.E.L., *Enlarged electrochemical window in dialkyl-imidazolium cation based room-temperature air and water-stable molten salts*. Electrochimica Acta, **42**(16): p. 2533-2535, 1997.
50. Lane, G.H., *Electrochemical reduction mechanisms and stabilities of some cation types used in ionic liquids and other organic salts*. Electrochimica Acta, **83**(0): p. 513-528, 2012.
51. Bond, A.M., Oldham, K.B., Snook, G.A., *Use of the Ferrocene Oxidation Process To Provide Both Reference Electrode Potential Calibration and a Simple Measurement (via Semiintegration) of the Uncompensated Resistance in Cyclic Voltammetric Studies in High-Resistance Organic Solvents*. Analytical Chemistry, **72**(15): p. 3492-3496, 2000.
52. Laszlo, J.A., Compton D.L.,  *$\alpha$ -Chymotrypsin catalysis in imidazolium-based ionic liquids*. Biotechnology and Bioengineering, **75**(2): p. 181-186, 2001.

53. Cammarata, L., Kazarian, S.G., Salter, P.A., Welton, T., *Molecular states of water in room temperature ionic liquids*. *Physical Chemistry Chemical Physics*, **3**(23): p. 5192-5200, 2001.
54. Clare, B.R., Bayley, P.M., Best, Adam S., Forsyth M., MacFarlane, D.R., *Purification or contamination? The effect of sorbents on ionic liquids*. *Chemical Communications*, (23): p. 2689-2691, 2008.
55. Nockemann, P., Binnemans, K., Driesen, K., *Purification of imidazolium ionic liquids for spectroscopic applications*. *Chemical Physics Letters*, 2005. **415**(1-3): p. 131-136.
56. Pallana, O.G., *Engineering Chemistry*. New Dehli: Tata McGraw-Hill Education, 2009.
57. Fulmer, G.R., Miller, A.J.M., Sherdend, N.H., Gottlieb, H.E., Nudelman, A., Stoltz, B.M., Bercaw, J.E., Goldberg, K. I., *NMR Chemical Shifts of Trace Impurities: Common Laboratory Solvents, Organics, and Gases in Deuterated Solvents Relevant to the Organometallic Chemist*. *Organometallics*, **29**(9): p. 2176-2179, 2010.
58. Silvester, D.C., Compton, R.G., *Electrochemistry in room temperature ionic liquids: A review and some possible applications*. *Journal of Research In Physical Chemistry*, **220**(10-11): p. 1247-1274, 2006.
59. Randström, S., Appetecchi, G.B., Lagergren, C., Moreno, A., Passerini, S., *The influence of air and its components on the cathodic stability of N-butyl-N-methylpyrrolidinium bis(trifluoromethanesulfonyl)imide*. *Electrochimica Acta*, **53**(4): p. 1837-1842, 2007.
60. Ue, M., Murakami, A., Nakamura, S., *Anodic Stability of Several Anions Examined by Ab Initio Molecular Orbital and Density Functional Theories*. *S. J. Electrochem. Soc.*, **149**: p. 1572-1577, 2002.
61. Galiński, M., Lewandowski, A., Stępiak, I., *Ionic liquids as electrolytes*. *Electrochimica Acta*, **51**(26): p. 5567-5580, 2006.
62. Buzzeo, M.C., Hardacre, C., Compton, R.G., *Extended Electrochemical Windows Made Accessible by Room Temperature Ionic Liquid/Organic Solvent Electrolyte Systems*. *ChemPhysChem*, **7**(1): p. 176-180, 2006.
63. Swatloski, R.P., Holbrey, J.D., Rogers, R.D., *Ionic liquids are not always green: hydrolysis of 1-butyl-3-methylimidazolium hexafluorophosphate*. *Green Chemistry*, **5**(4): p. 361-363, 2003.

# Annex 1

TFSI and NTf<sub>2</sub> are the same anion.

Ionic liquid	Working electrode	Reference electrode	Cathodic limiting potential, $E_{CL}$ (V)		Anodic limiting potential, $E_{AL}$ (V)		Electrochemical window (V)	Reference
			vs. RE	vs. Fe/Fe <sup>+</sup>	vs. RE	vs. Fe/Fe <sup>+</sup>		
[BMIm]BF <sub>4</sub>	Ag	Pt QRE	-1.75		1.25		4.20	[42]
[BMIm]BF <sub>4</sub>	Au	Ag QRE	-2.20		2.40		4.60	[43]
[BMIm]BF <sub>4</sub>	Au RED <sup>3)</sup>	Pt QRE	-1.85		2.23		4.20	[36]
[BMIm]BF <sub>4</sub>	GC			-2.55		2.13	4.68	[24]
[BMIm]BF <sub>4</sub>	GC	Ag QRE	-2.20		2.20		4.40	[43]
[BMIm]BF <sub>4</sub>	GC	Li/Li <sup>+</sup>	0.80		5.40		4.60	[44]
[BMIm]BF <sub>4</sub>	GC RED	Pt QRE	-1.80		3.65		5.45	[36]
[BMIm]BF <sub>4</sub>	Pt	Mg/Mg <sup>+</sup>	-1.50		1.50		3.00	[44]
[BMIm]BF <sub>4</sub>	Ni	Pt QRE	<1.55		0.80		>2.23	[42]
[BMIm]BF <sub>4</sub>	Pt			-2.80		2.30	5.10	[38]
[BMIm]BF <sub>4</sub>	Pt	Ag/Ag <sup>+</sup>	-1.80		2.40		4.20	[27]
[BMIm]BF <sub>4</sub>	Pt	Ag QRE	-2.40		2.50		4.90	[43]
[BMIm]BF <sub>4</sub>	Pt	Mg/Mg <sup>+</sup>	-1.25		>1.5		>2.75	[43]
[BMIm]NTf <sub>2</sub>	Au micro	Ag QRE	-2.04		2.72		4.76	[34]
[BMIm]NTf <sub>2</sub>	GC			-2.50		2.12	4.62	[24]
[BMIm]NTf <sub>2</sub>	GC	Pt QRE	-2.4		2.5		4.9	This work
[BMIm]NTf <sub>2</sub>	Pt			-2.70		2.30	5.00	
[BMIm]NTf <sub>2</sub>	Pt	Ag/Ag <sup>+</sup>	-2.00		2.60		4.60	[29]
[BMIm]PF <sub>6</sub>	Au	Pt QRE	-2.20		2.30		4.50	[47]
[BMIm]PF <sub>6</sub>	Au RED	Pt QRE	-2.50		3.45		5.95	[36]
[BMIm]PF <sub>6</sub>	GC RED	Pt QRE	-2.50		3.85		6.23	[36]
[BMIm]PF <sub>6</sub>	Pt			-2.90		2.10	5.00	[38]
[BMIm]PF <sub>6</sub>	Pt	Ag/Ag <sup>+</sup>	-1.90		2.50		4.40	[29]
[BMIm]PF <sub>6</sub>	Pt	Ag QRE	-1.10		2.10		3.20	[29]
[BMIm]PF <sub>6</sub>	Pt micro	Ag QRE	-2.00		1.70		3.70	[14]
[BMIm]PF <sub>6</sub>	Pt micro	Pt QRE	-1.60		2.55		4.15	[45]
[BMIm]PF <sub>6</sub>	Pt RED	Pt QRE	-2.30		3.40		5.70	[36]
[BMIm]PF <sub>6</sub>	Pt ume	Pt QRE	-2.00		3.00		5.00	[36]
[BMIm]PF <sub>6</sub>	W RED	Pt QRE	-2.10		5.00		7.10	[36]

Figure 22. State of the art of the electrochemical windows of ILs.

## Annex 2

*Table 11. Summary of the final anion substitution reaction appearance, extraction method and final IL appearance.*

Product	Final reaction appearance	Extraction method	Final product appearance
[BMIm][TFSI]	Two phases	Decantation	Slightly viscous, transparent liquid
[BnMIm][TFSI]	Two phases	Decantation	Slightly viscous, transparent liquid
[Bn <sup>F</sup> MIm][TFSI]	Milky foam	Vacuum filtration	White Crystalline
[BMIm][PF <sub>6</sub> ]	Two phases	Decantation after add DCM	Liquid with some white crystals
[BnMIm][PF <sub>6</sub> ]	Two phases	Decantation after add DCM	White Crystalline
[Bn <sup>F</sup> Mim][PF <sub>6</sub> ]	Milky foam	Vacuum filtration	White Crystalline
[BnMIm][BF <sub>4</sub> ]	Two phases	Decantation after adding DCM	Yellowed white crystalline

## Annex 3

In this annex the NMR spectrum of the different ionic liquids is made available.

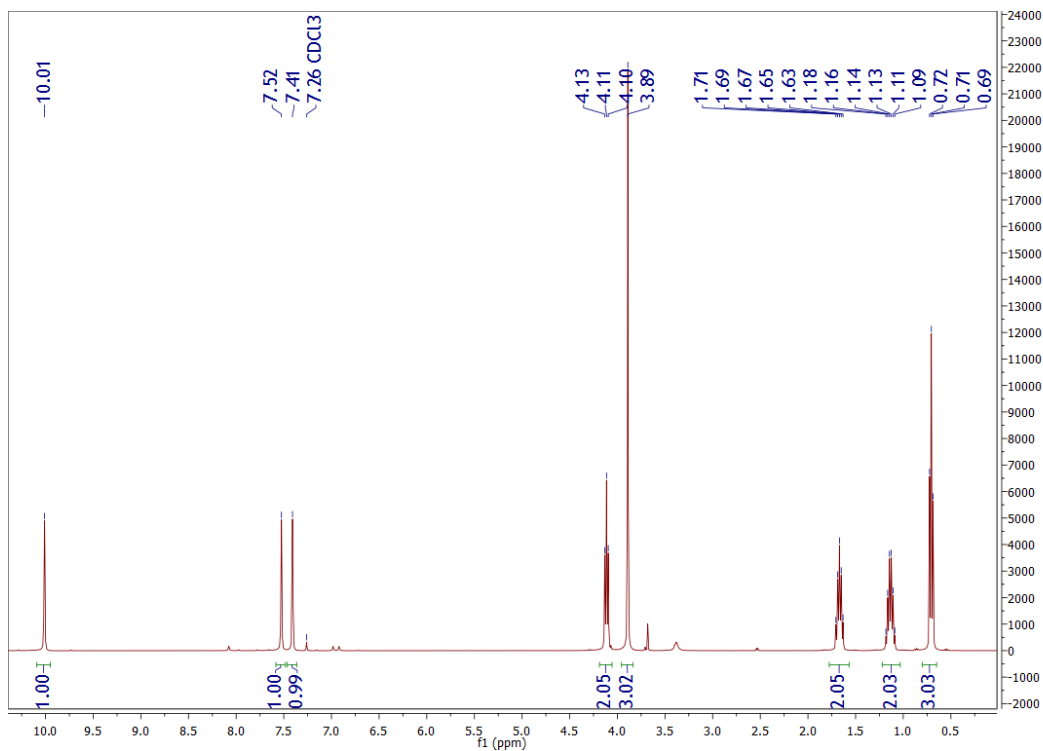


Figure 23. NMR spectrum of [BMIm][Br] <sup>1</sup>H.

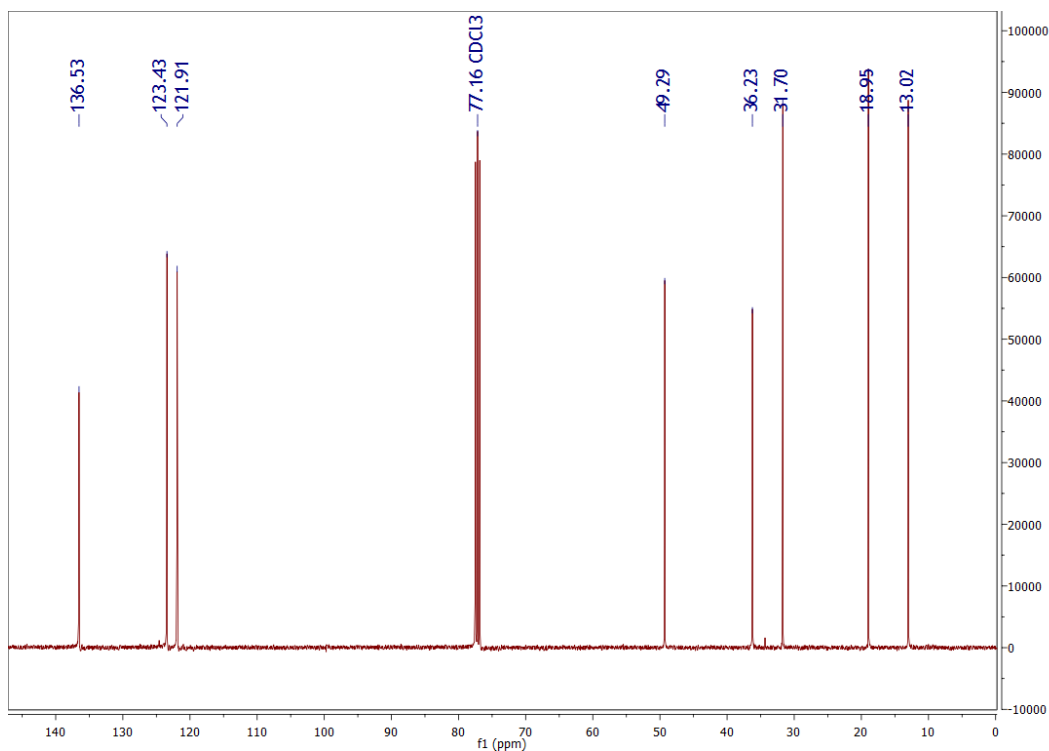
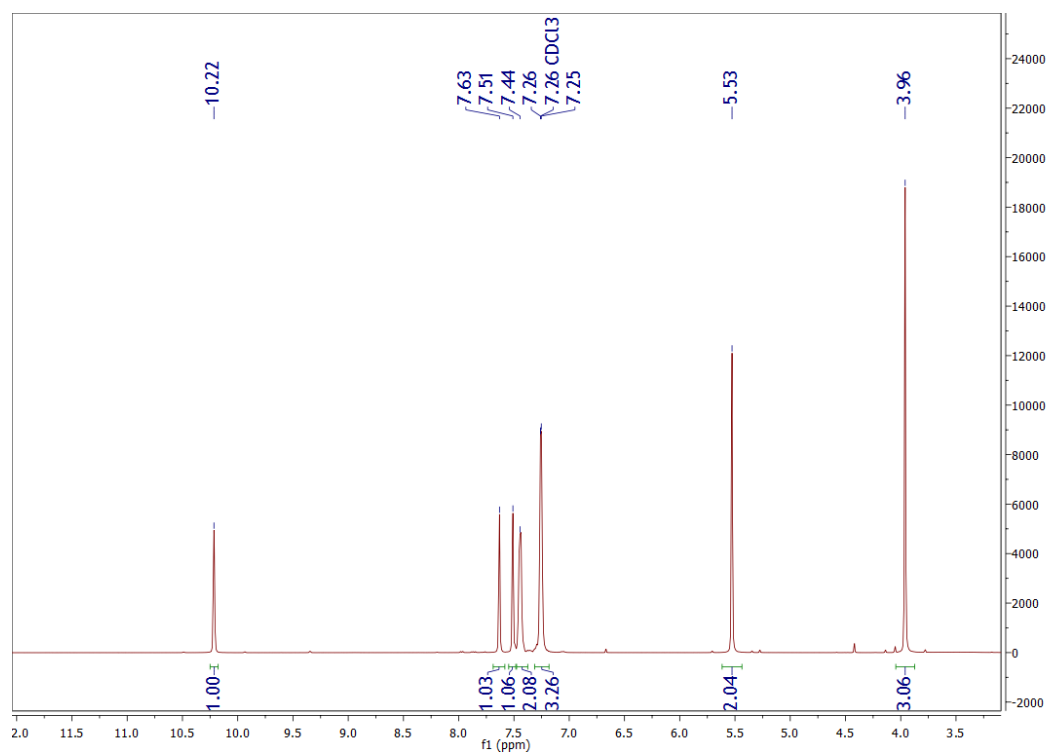
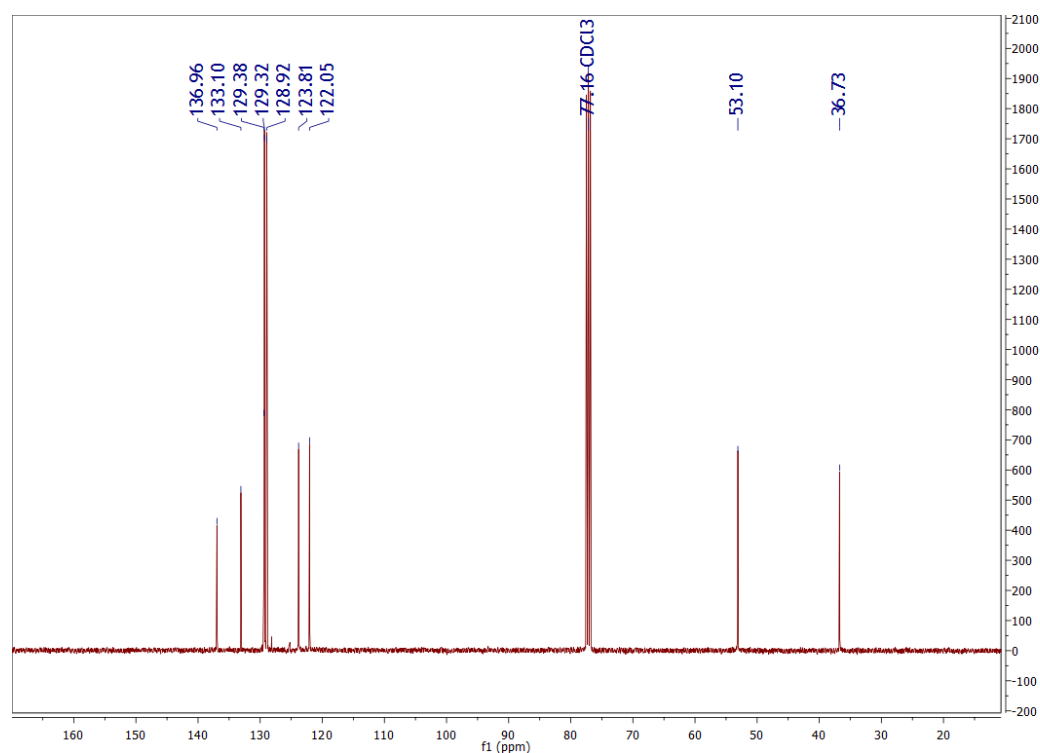


Figure 24. NMR spectrum of [BMIm][Br] <sup>13</sup>C.


 Figure 25. NMR spectrum of [BnMIm][Br] <sup>1</sup>H.

 Figure 26. NMR spectrum of [BnMIm][Br] <sup>13</sup>C.

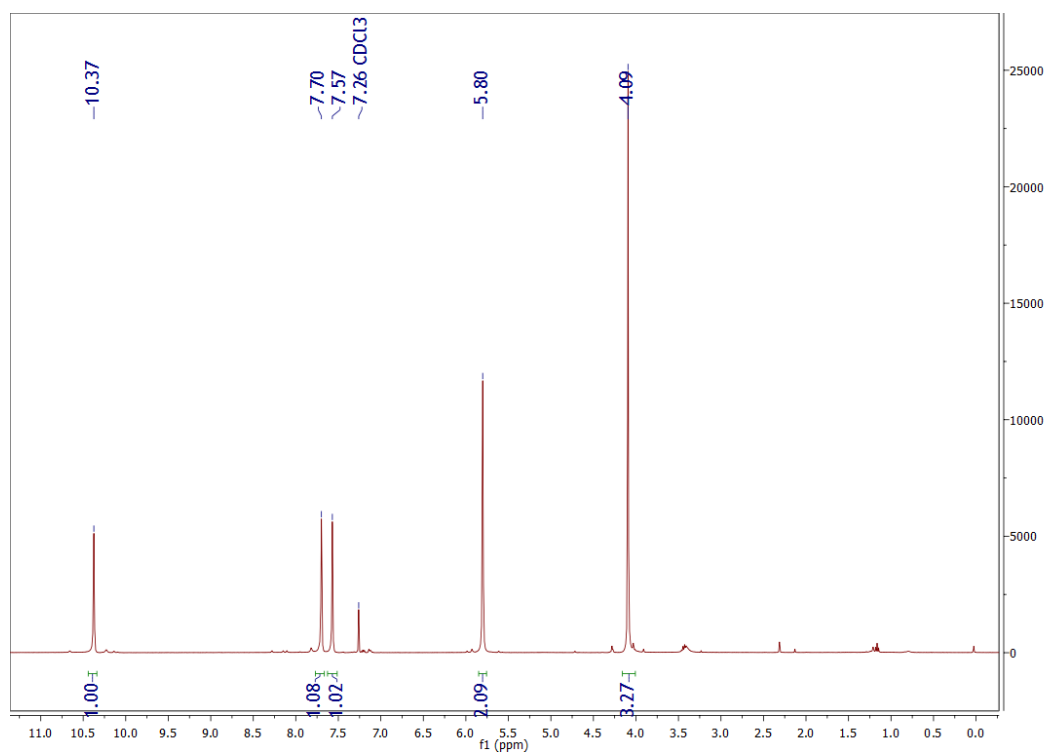


Figure 27. NMR spectrum of  $[\text{Bn}^{\text{F}}\text{MIm}][\text{Br}]$   $^1\text{H}$ .

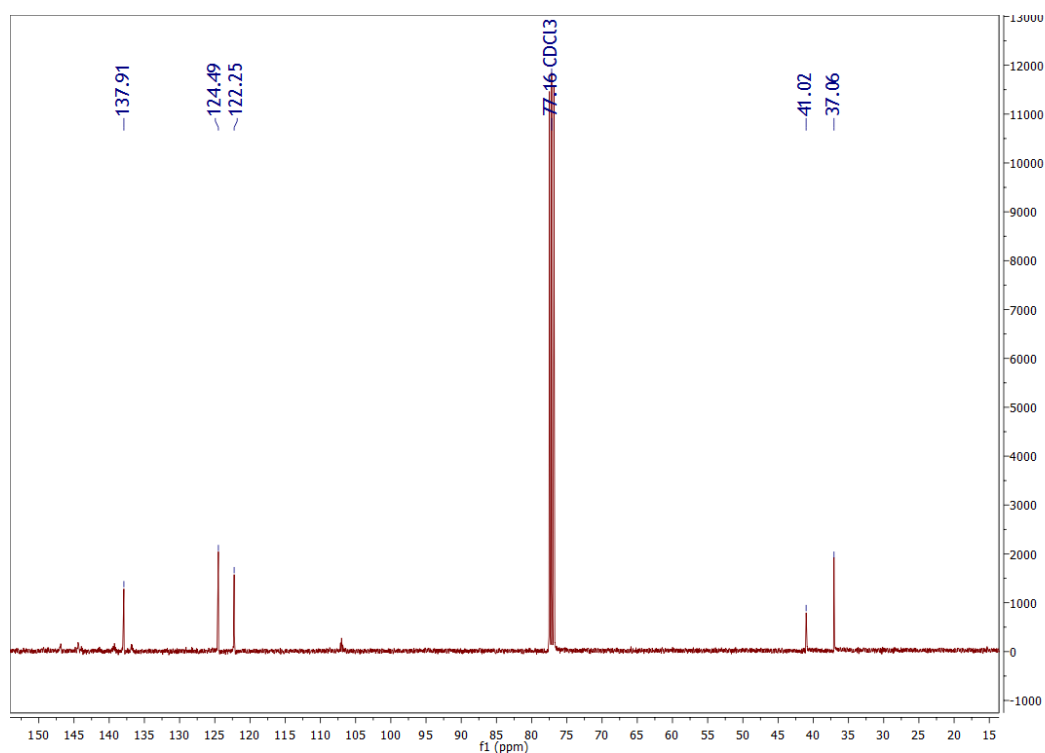


Figure 28. NMR spectrum of  $[\text{Bn}^{\text{F}}\text{MIm}][\text{Br}]$   $^{13}\text{C}$ .



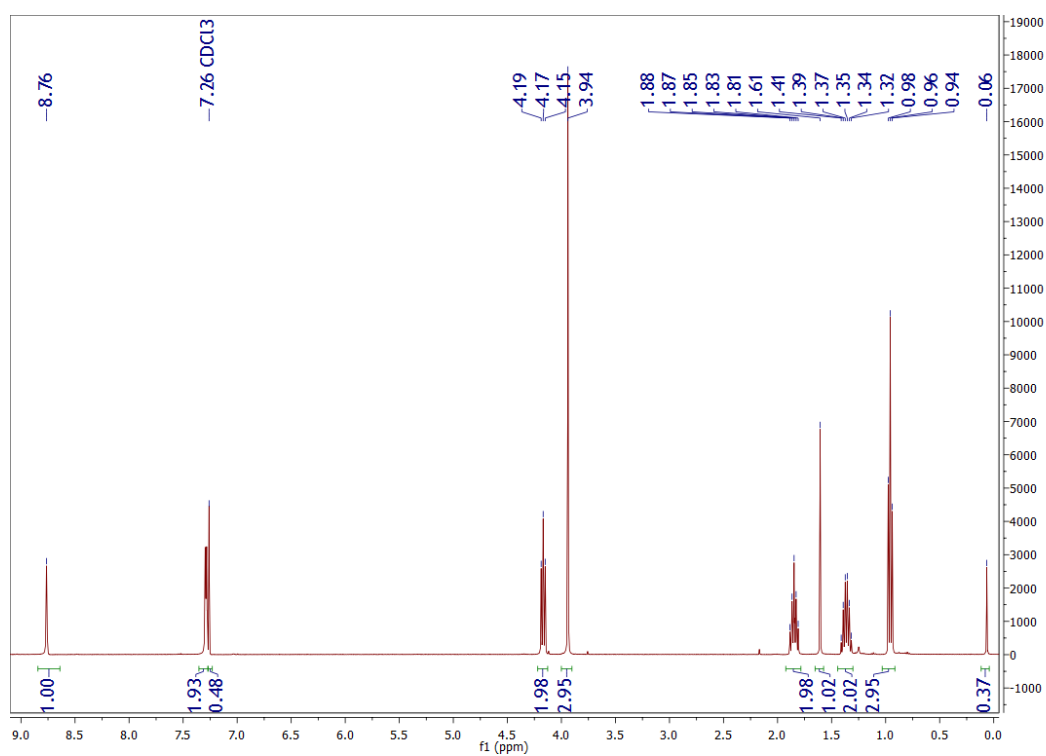


Figure 29. NMR spectrum of  $[\text{BMIm}][\text{TFSI}]$   $^1\text{H}$ .

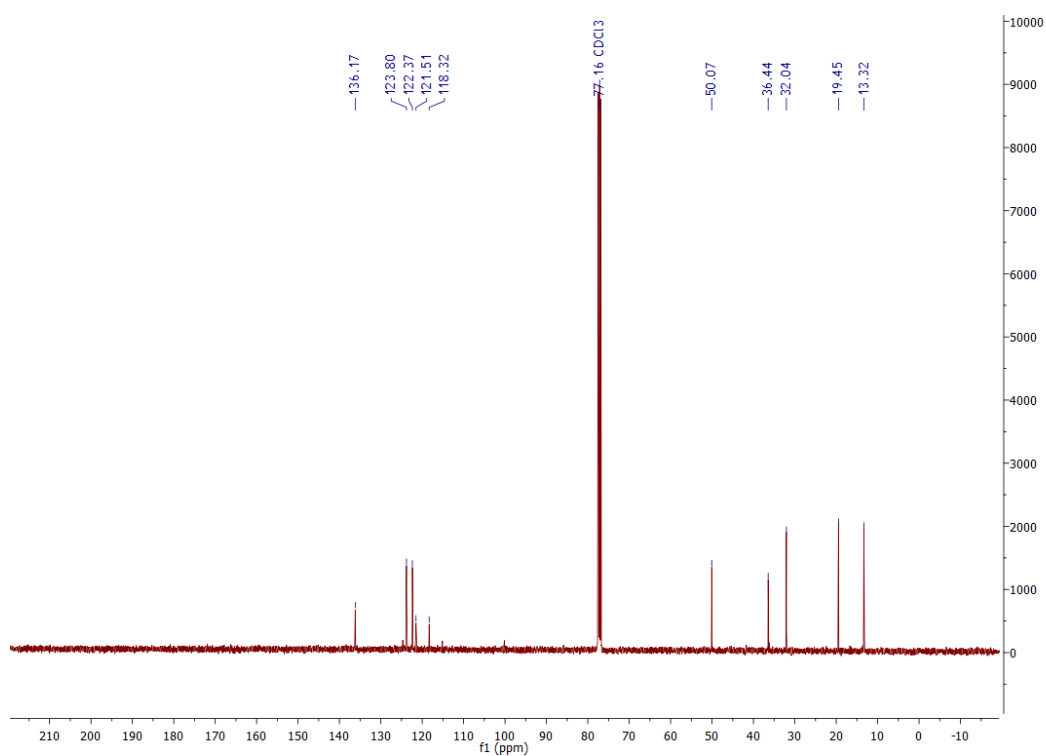
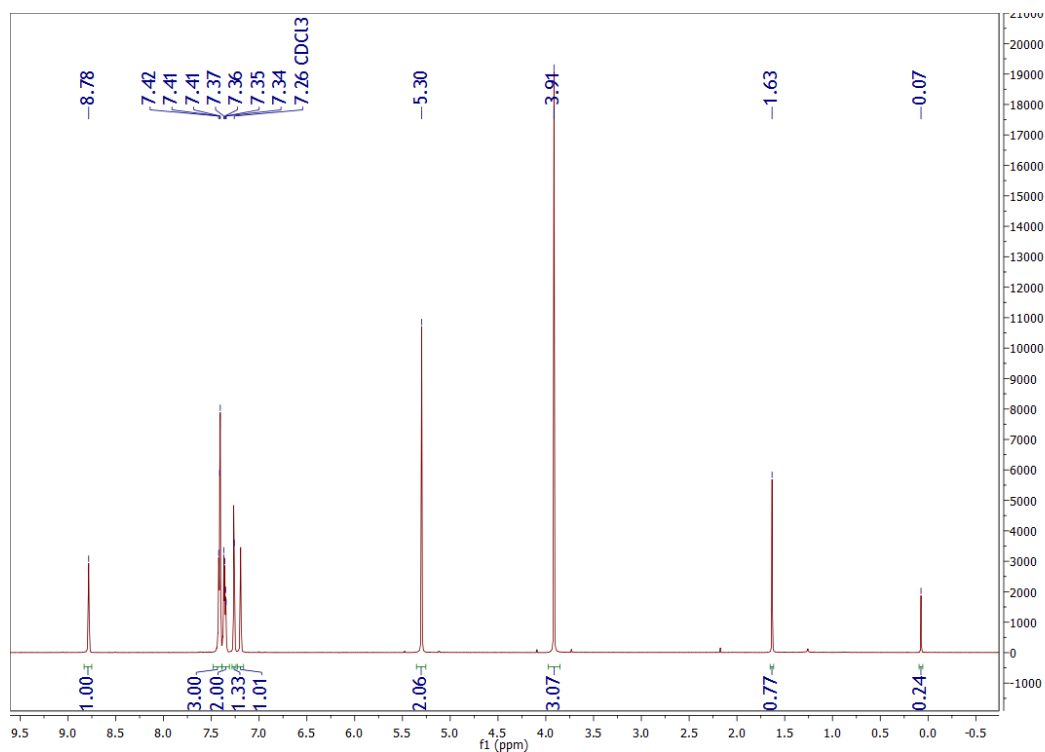
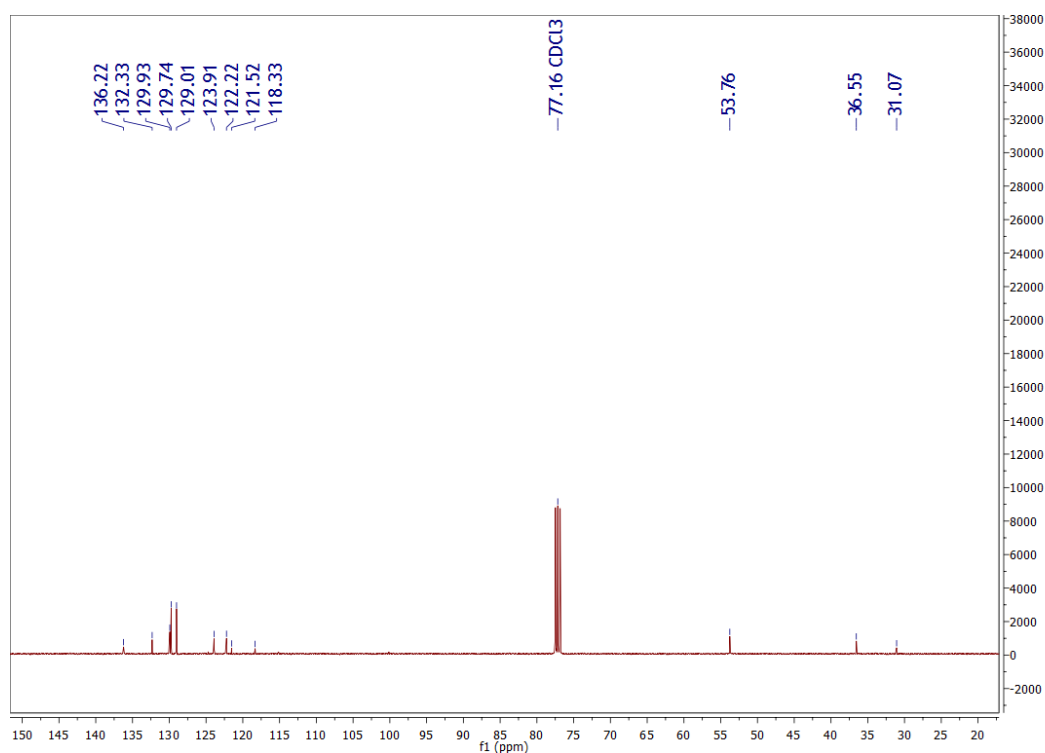
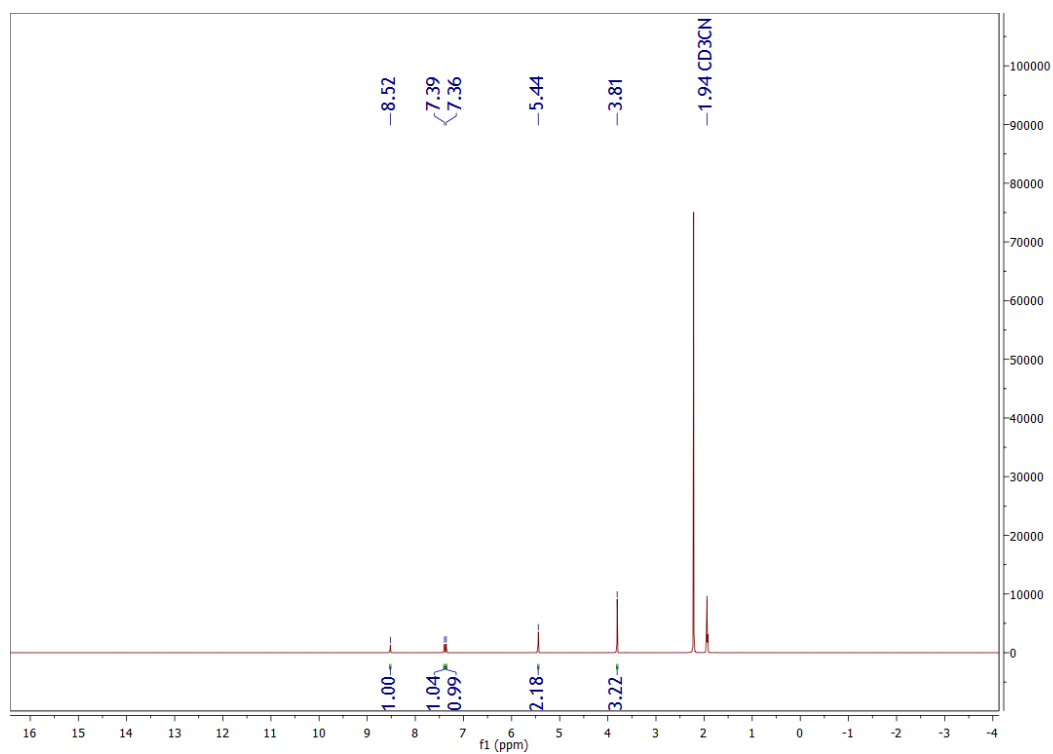
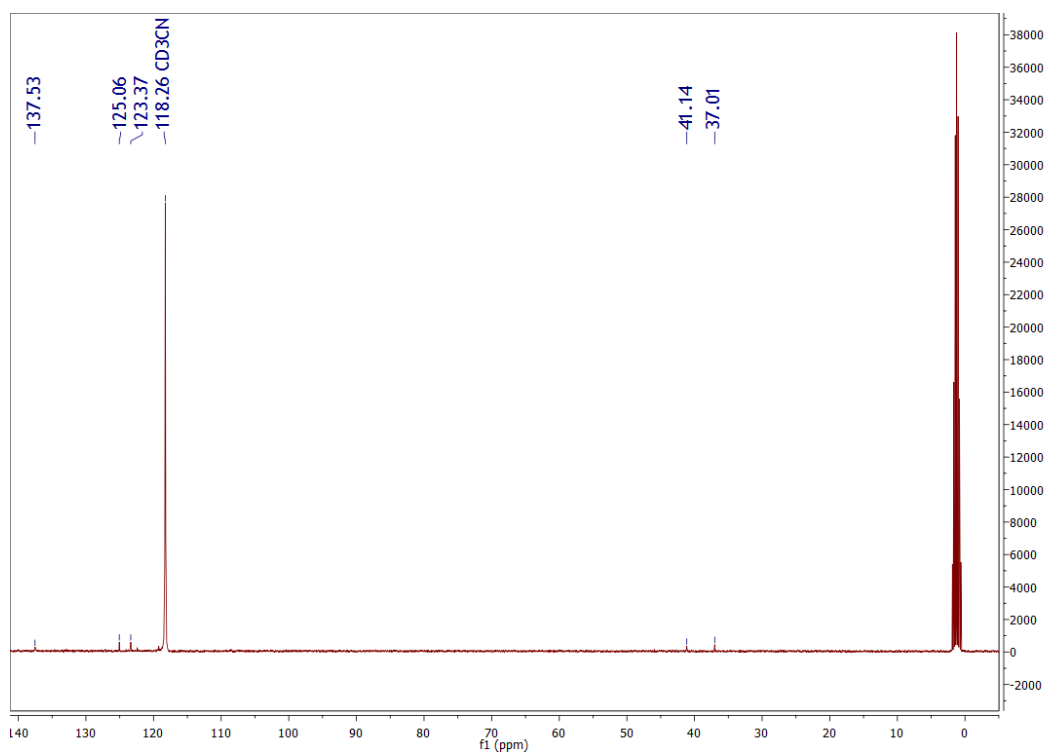
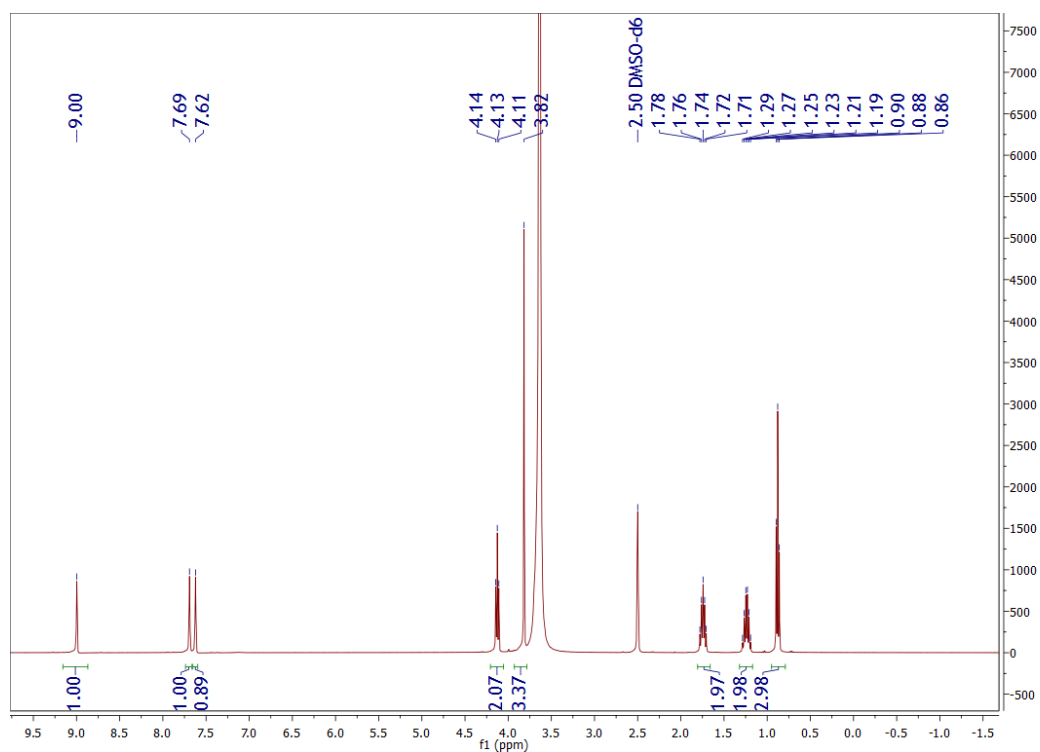
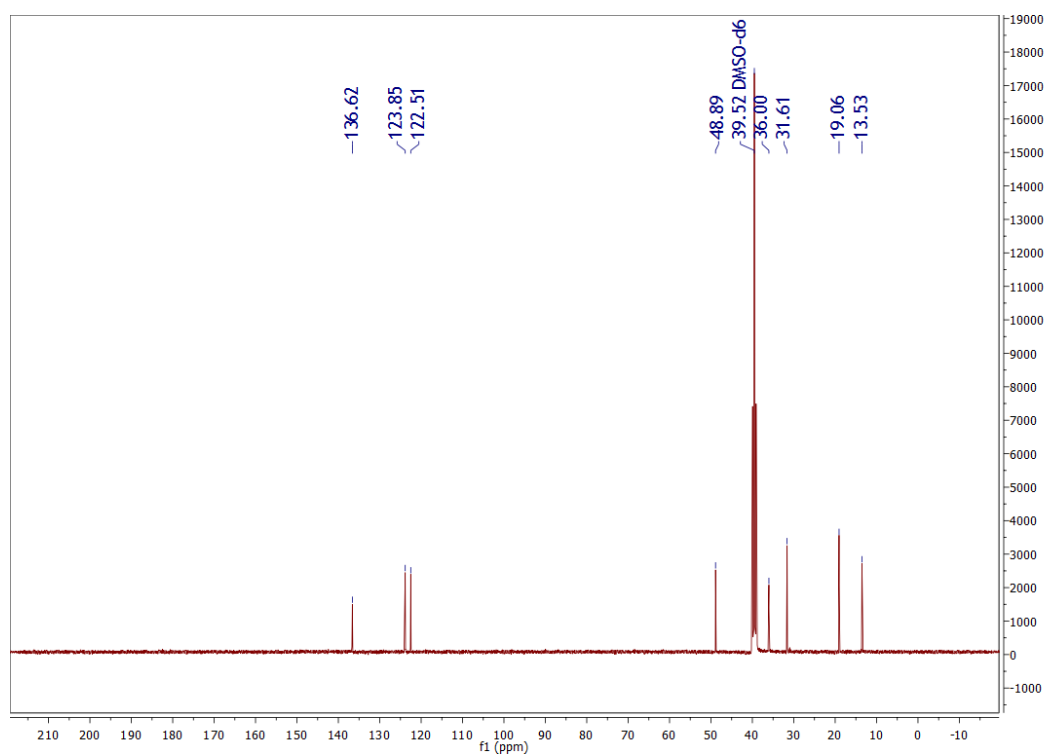


Figure 30. NMR spectrum of  $[\text{BMIm}][\text{TFSI}]$   $^{13}\text{C}$ .


 Figure 31. NMR spectrum of [BnMIm][TFSI] <sup>1</sup>H.

 Figure 32. NMR spectrum of [BnMIm][TFSI] <sup>13</sup>C.


 Figure 33. NMR spectrum of [Bn<sup>F</sup>MIm][TFSI] <sup>1</sup>H.

 Figure 34. NMR spectrum of [Bn<sup>F</sup>MIm][TFSI] <sup>13</sup>C.


 Figure 35. NMR spectrum of  $[\text{BMIm}][\text{PF}_6]$   $^1\text{H}$ .

 Figure 36. NMR spectrum of  $[\text{BMIm}][\text{PF}_6]$   $^{13}\text{C}$ .

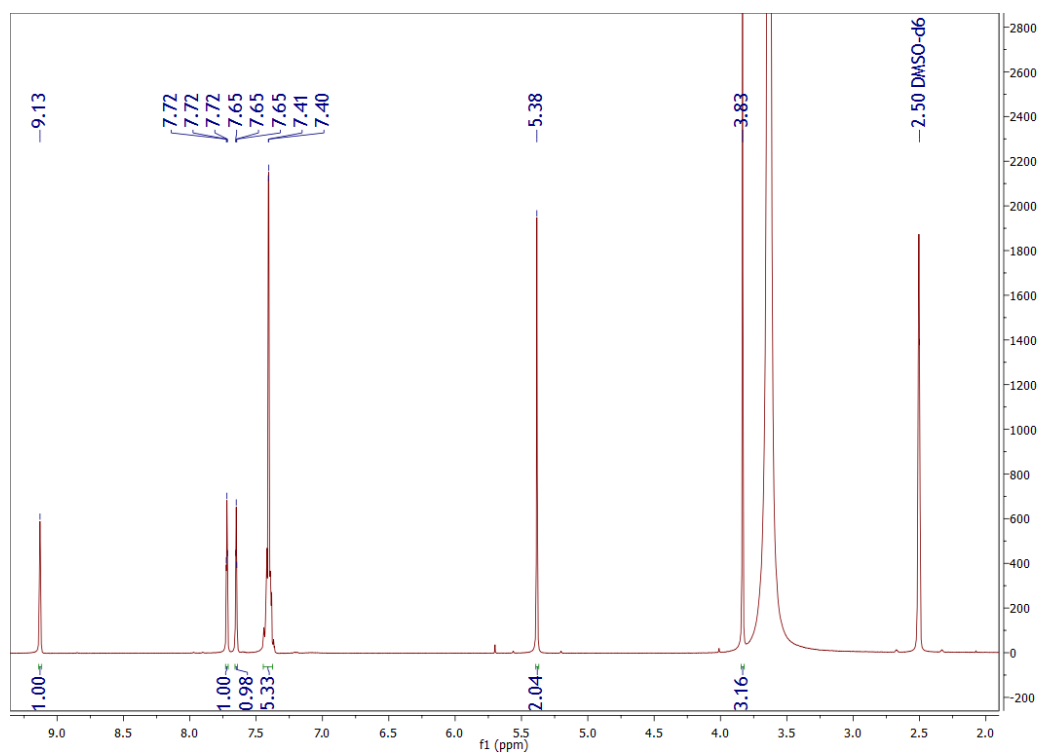


Figure 37. NMR spectrum of  $[\text{BnMIm}][\text{PF}_6]$   $^1\text{H}$ .

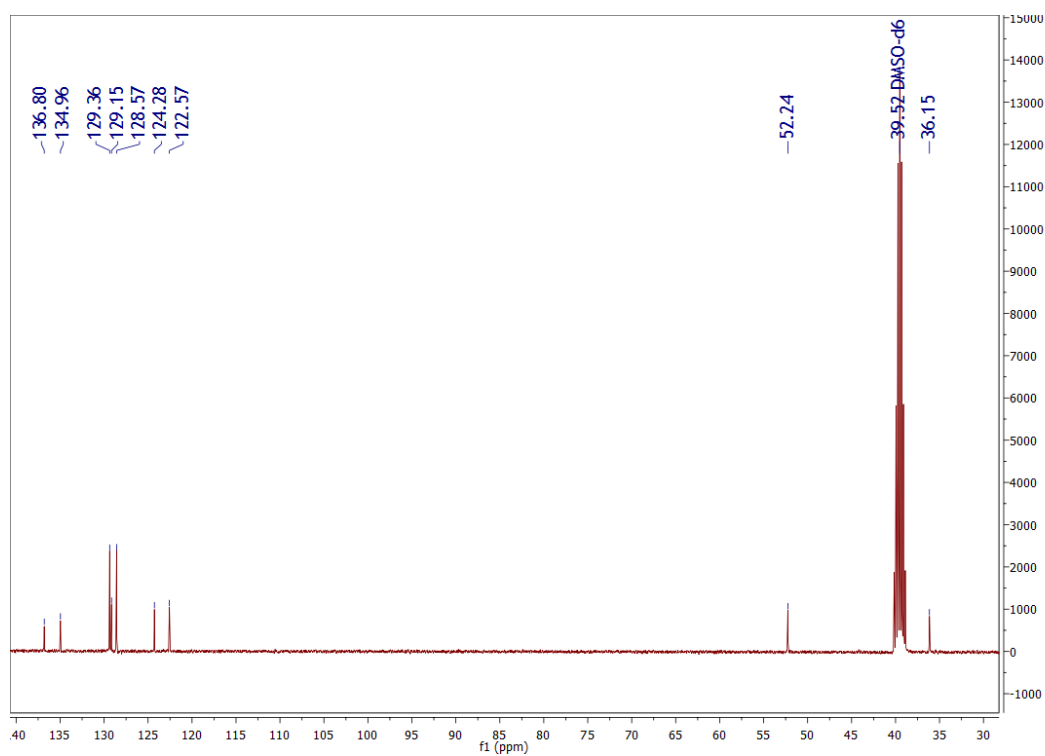
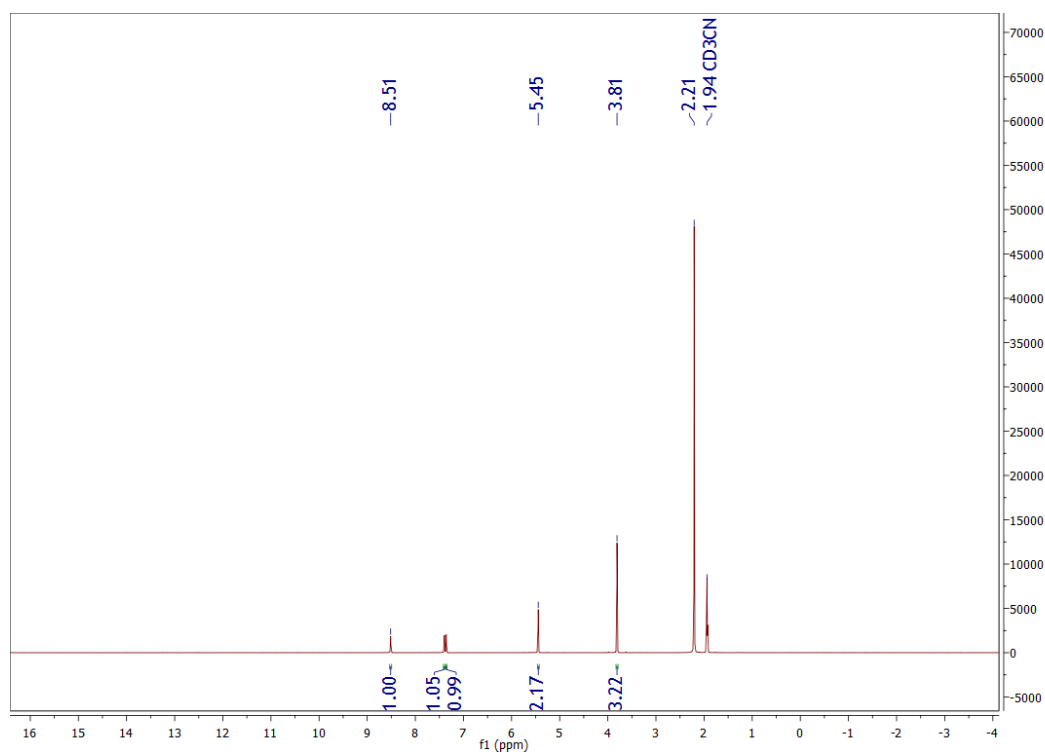
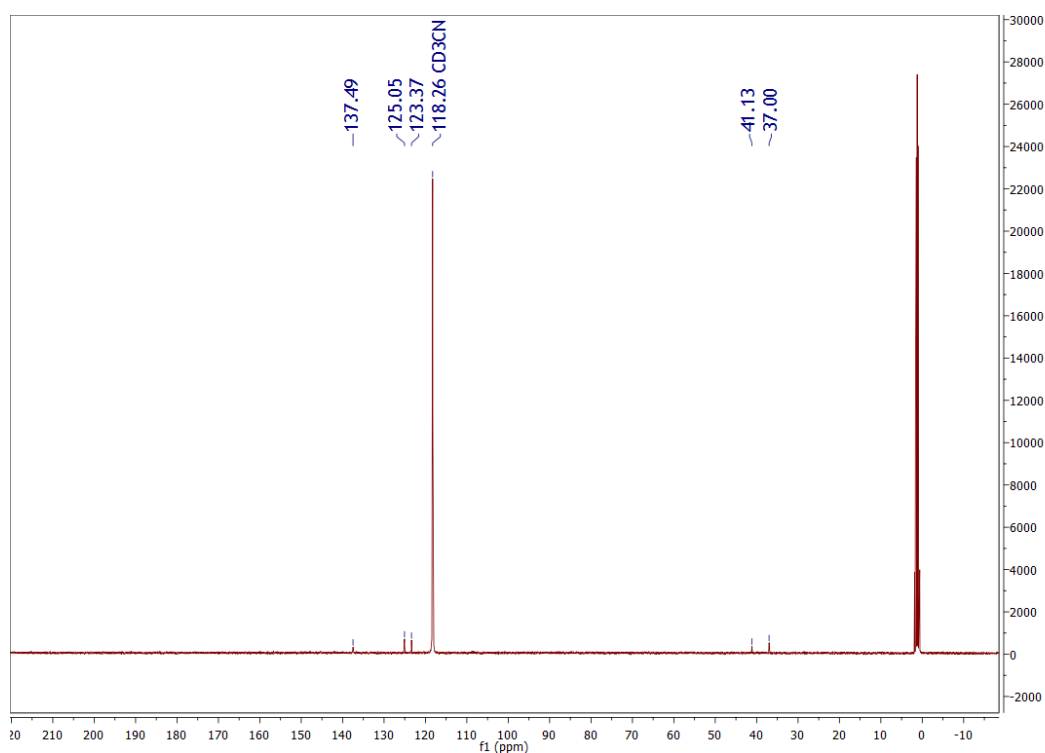
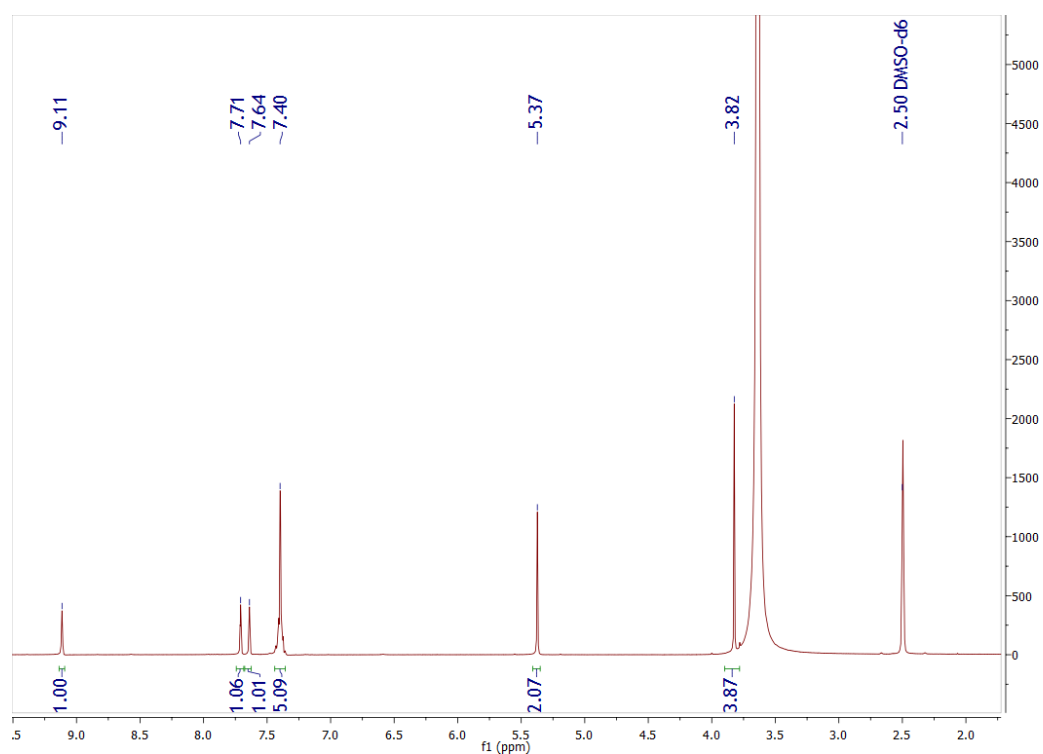
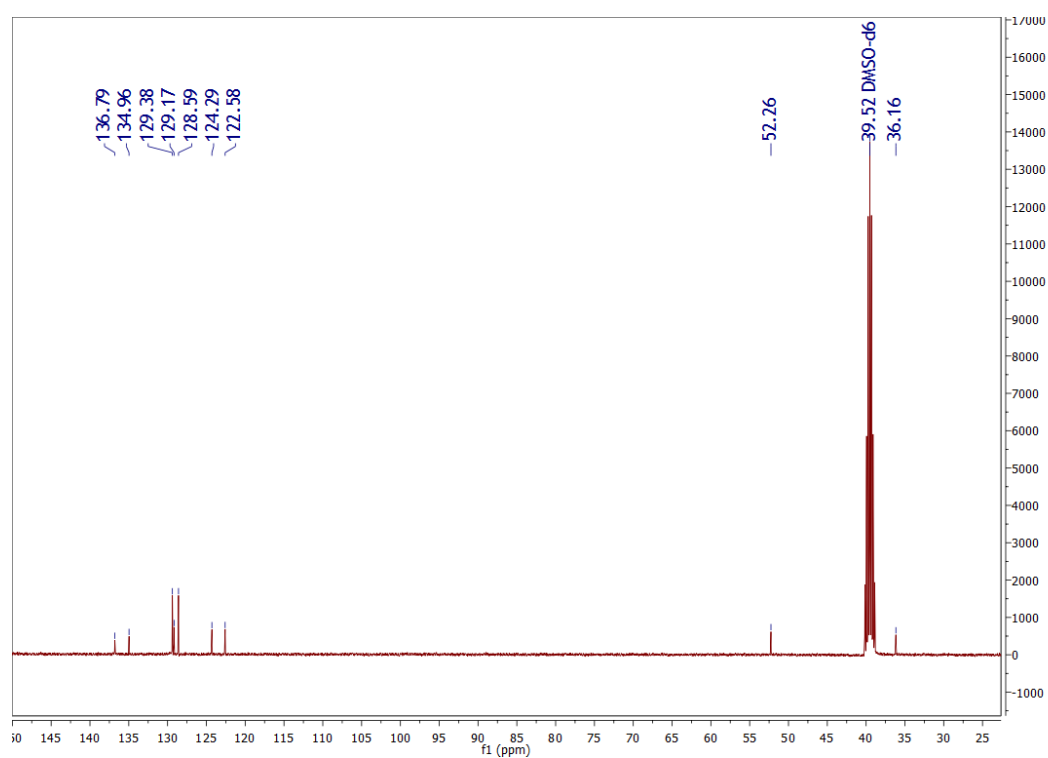


Figure 38. NMR spectrum of  $[\text{BnMIm}][\text{PF}_6]$   $^{13}\text{C}$ .


 Figure 39. NMR spectrum of  $[\text{Bn}^{\text{F}}\text{MIm}][\text{PF}_6]$   $^1\text{H}$ .

 Figure 40. NMR spectrum of  $[\text{Bn}^{\text{F}}\text{MIm}][\text{PF}_6]$   $^{13}\text{C}$ .


 Figure 41. NMR spectrum of [BnMIm][BF<sub>4</sub>]<sup>1</sup>H.

 Figure 42. NMR spectrum of [BnMIm][BF<sub>4</sub>]<sup>13</sup>C.

## Annex 4

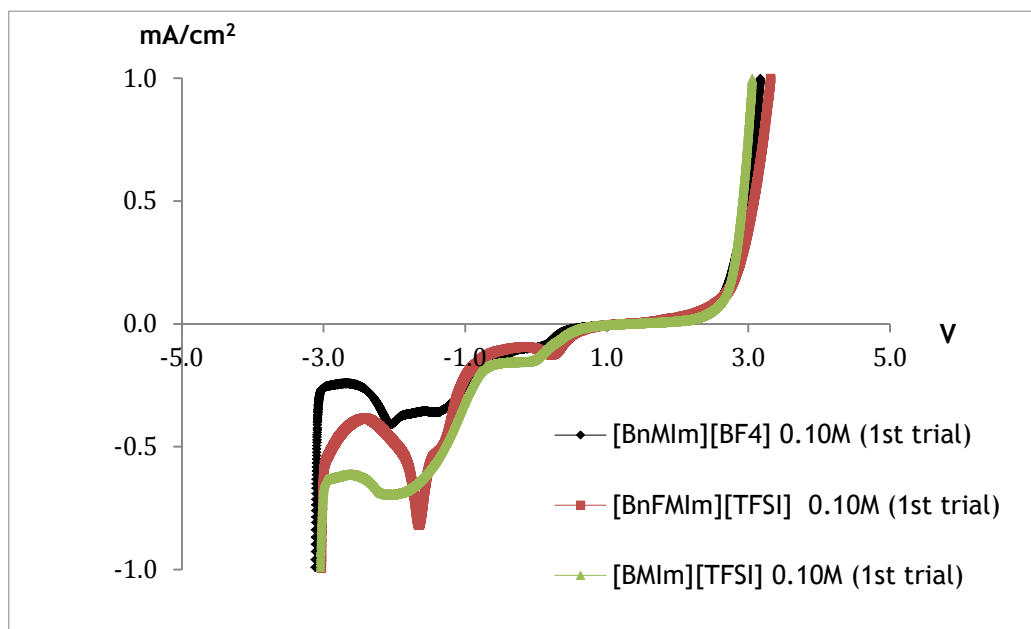


Figure 43. EWs comparison between [BnMIm][BF<sub>4</sub>], [BnFMIm][TFSI] and [BMIm][TFSI].



Table 12. Full LSV results

Ionic Liquid	CL(V)		ALV)		EWs	
	Vs. Ag QRE		Vs. Ag QRE			
	1 <sup>st</sup> trial	2 <sup>nd</sup> trial	1 <sup>st</sup> trial	2 <sup>nd</sup> trial	1 <sup>st</sup> trial	2 <sup>nd</sup> trial
Blank	-3.19	-3.23	2.98	2.93	6.17	6.16
[BmIm][TFSI] 0.1 M	-3.04	-3.04	3.06	3.03	6.10	6.07
[BmIm][TFSI] 0.25 M	<del>-4.73</del>	-3.21	<del>2.99</del>	3.02	<del>4.72</del>	6.23
[BnMIm][TFSI] 0.1 M	-2.86	-3.19	3.19	3.04	6.05	6.23
[BnMIm][TFSI] 0.25 M	-3.14	<del>-4.24</del>	3.04	<del>3.04</del>	6.18	<del>4.22</del>
[Bn <sup>F</sup> MIm][TFSI] 0.1 M	-3.02	-3.22	3.32	3.21	6.34	6.43
[Bn <sup>F</sup> MIm][TFSI] 0.25 M	-3.16	-3.20	3.10	3.06	6.26	6.26
[BmIm][PF <sub>6</sub> ] 0.1 M	-3.07	-3.10	3.00	3.00	6.07	6.10
[BmIm][PF <sub>6</sub> ] 0.25 M	-2.84	-3.20	3.05	2.95	5.89	6.15
[BnMIm][PF <sub>6</sub> ] 0.10 M	-3.09	-3.40	3.16	3.65	6.25	7.05
[BnMIm][PF <sub>6</sub> ] 0.25 M	-3.26	-3.09	3.05	3.01	6.31	6.10
[Bn <sup>F</sup> MIm][PF <sub>6</sub> ] 0.10 M	-3.20	-3.25	3.19	3.25	6.39	6.50
[Bn <sup>F</sup> MIm][PF <sub>6</sub> ] 0.25 M	-3.22	-3.26	3.05	3.24	6.27	6.50
[BnMIm][BF <sub>4</sub> ] 0.10 M	-3.12	3.19	3.18	3.14	6.30	6.33
[BnMIm][BF <sub>4</sub> ] 0.25 M	-3.21	-3.09	3.16	3.01	6.37	6.53